

# **Infrared Emitters and Detectors Data Book**

**1994**

**TEMIC**  
TELEFUNKEN Semiconductors

## General Information

<b>1.</b>	<b>Selector guide</b>	<b>11</b>
1.1	Alpha-numeric index	11
1.2	IR emitters	12
1.3	Detectors	14
1.4	Photomodules	17
1.5	IrDA-infrared data transmission	18
<b>2.</b>	<b>Explanation of technical data</b>	<b>19</b>
2.1	Type designation code for semiconductor devices according to Pro Electron	19
2.2	TEMIC Type designation systems	20
<b>3.</b>	<b>Data sheet illustration</b>	<b>21</b>
3.1	Symbols and terminology	21
3.2	Data sheet construction	29
3.2.1	Device description	29
3.2.2	Absolute maximum ratings	29
3.2.3	Thermal data – thermal resistances	29
3.2.4	Basic characteristics	30
3.2.5	Family of curves	30
3.2.6	Dimensions (Mechanical data)	30
<b>4.</b>	<b>Physics and technology</b>	<b>31</b>
4.1	Emitters	31
4.1.1	Materials	31
4.1.2	IREM chips and characteristics	31
4.2	UV, visible, and near IR silicon photodetectors	34
4.2.1	Silicon photodiodes	34
4.2.1.1	The physics of silicon detector diodes	34
4.2.2	Properties of silicon photodiodes	35
4.2.2.1	I-V Characteristics of illuminated pn junction	35
4.2.2.2	Spectral responsivity	36
4.2.2.2.1	Efficiency of Si photodiodes	36
4.2.2.2.2	Temperature dependence of spectral responsivity	37
4.2.2.2.3	Uniformity of spectral responsivity	37
4.2.2.2.4	Stability of spectral responsivity	37
4.2.2.2.5	Angular dependence of responsivity	37
4.2.2.3	Dynamic properties of Si photodiodes	38
4.2.3	Characteristics of other silicon photodetectors	38
4.2.3.1	Avalanche photodiodes	38
4.2.3.2	Phototransistors	38

## Table of Contents

4.2.4	Applications	39
4.2.4.1	Equivalent circuit	39
4.2.4.2	Searching for the right detector diode type	39
4.2.4.3	Operating modes and circuits	41
4.2.4.4	Frequency response	41
4.2.4.5	Which type for which application?	43
4.2.5	Phototransistors	43
4.2.5.1	Circuits	43
<b>5.</b>	<b>Measurement techniques</b>	<b>44</b>
5.1	Introduction	44
5.2	Dark and light measurements	44
5.2.1	Emitter devices	44
5.2.1.1	IR diodes (GaAs)	44
5.2.1.2	Light emitting diodes	45
5.2.2	Detector devices	46
5.2.2.1	Photovoltaic cells, photodiodes	46
5.2.2.2	Phototransistors, photodarlington transistors	47
5.2.3	Coupling devices	48
5.3	Switching characteristics	49
5.3.1	Definition	49
5.3.2	Notes concerning the test set-up	49
5.3.3	Switching characteristic improvements on phototransistors and darlington phototransistors	49
<b>6.</b>	<b>Component construction</b>	<b>50</b>
<b>7.</b>	<b>Tape and reel standards</b>	<b>51</b>
7.1.	Packing	51
7.1.1	Number of components	51
7.1.2.	Missing components	51
7.2	Order designation	51
7.2.1	Tape dimensions for $\varnothing$ 3 mm standard packages	52
7.2.2	Tape dimensions for $\varnothing$ 5 mm standard packages	53
7.2.3	Reel package, dimensions in mm	54
7.2.4	Fan-fold packing	56
7.3	Taping of SMT-devices	57
7.3.1	Number of components	58
7.3.2	Missing devices	59
7.3.3	Top tape removal force	59
7.3.4	Ordering designation	59

<b>8.</b>	<b>Assembly instructions</b>	<b>60</b>
8.1	General	60
8.2	Soldering instructions	60
8.3	Heat removal	62
8.4	Cleaning	63
8.5	Warning	63
<b>9.</b>	<b>Quality information</b>	<b>64</b>
9.1	Quality management	64
9.1.1	TEMIC continuous improvement activities	64
9.1.2	TEMIC tools for continuous improvement	64
9.1.3	TEMIC quality policy	64
9.2	General quality flow chart diagram	65
9.2.2	Production flow chart diagram	66
9.3	Qualification and monitoring	67
9.3.1	Qualification procedure	67
9.3.2	Quality indicators	67
9.4	Failure rates: FIT	67
9.5	Degradation of IREDs	68
9.6	Safety	68
9.6.1	Reliability and safety	68
9.6.2	Toxicity	68
9.6.3	Safety aspects of IR radiation	68
<b>Technical Data</b>		
	<b>Infrared Emitters</b>	<b>69</b>
	<b>Photodetectors</b>	<b>231</b>
	<b>Photomodules for PCM Remote Control Systems</b>	<b>479</b>
	<b>Infrared Data Transmission</b>	<b>493</b>
	<b>Addresses</b>	<b>519</b>

## 1. Selector guide

### 1.1 Alpha-numeric index

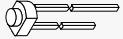
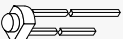


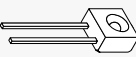
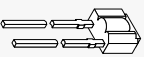

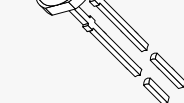
<b>B</b>					
BP 104	233	BPW 97	369	TEMT 4700	461
BPV 10	245	BPX 38	379	TEST 2500	467
BPV 10 F	237	BPX 43	385	TEST 2600	473
BPV 10 NF	241, 503	BPX 99 R	391	TFDS 3000	513
BPV 11	255			TFMS 5..0	481
BPV 11 F	249	<b>C</b>		TFMT 5..0	487
BPV 20 F	261	CQX 19	71	TSCA 6000	89
BPV 20 NFL	265	CQX 48	75	TSHA 440.	95
BPV 21 F	269	CQY 36 N	81	TSHA 520.	101
BPV 22 F	273	CQY 37 N	85	TSHA 550.	107, 495
BPV 22 NF	277, 505			TSHA 620.	113
BPV 23 F	281	<b>I</b>		TSHA 650.	119
BPV 23 NF	285, 507	IrDA Evaluation Kit	509	TSHF 5400	125, 499
BPV 23 NFL	289			TSIP 440.	129
BPW 13	293	<b>S</b>		TSIP 520.	135
BPW 14 N	297	S 153 P	395	TSIP 760.	141
BPW 16 N	301	S 186 P	399	TSMS 3700	147, 151
BPW 17 N	307	S 239 P	403	TSSA 2500	157
BPW 20 R	313	S 254 P N	407	TSSA 4500	163, 497
BPW 21 R	317	S 268 P	411	TSSF 4500	167, 501
BPW 24 R	321	S 289 P	417	TSSP 4400	171
BPW 34	325	S 350 P	421	TSSS 2600	177
BPW 41 N	329	S 351 P	427	TSTA 7100	183
BPW 43	333			TSTA 7300	187
BPW 46	337	<b>T</b>		TSTA 7500	191
BPW 76	375	TEFT 4300	433	TSTS 710.	195
BPW 77 N	341	TEMD 2100	439	TSTS 730.	199
BPW 78	345	TEMT 2100	443	TSTS 750.	203
BPW 82	351	TEMT 2200	449	TSUS 4300	207
BPW 83	355	TEMT 370.	455	TSUS 4400	213
BPW 85	359			TSUS 520.	219
BPW 96	365			TSUS 540.	225

## 1.2 IR emitters

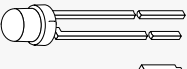

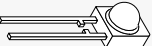
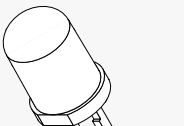
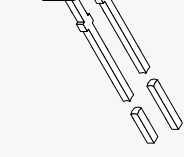
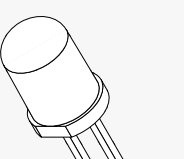
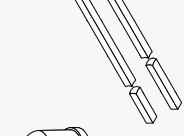

### Infrared emitting diodes

Package	Type	Characteristics					
		+/- φ	t <sub>r</sub> , t <sub>f</sub> / ns	I <sub>e</sub> / mW/sr @	I <sub>F</sub> / mA	V <sub>F</sub> / V @	I <sub>F</sub> / mA

#### IR emitter GaAs (950 nm) in plastic package

	CQY 36 N	40°	400	1.5(>0.7)	50	1.2(<1.6)	50
	CQY 37 N	12°	400	4.5(>2.2)	50	1.2(<1.6)	50
	TSUS 4300	20°	400	18(>7)	100	1.3(<1.7)	100
	TSUS 4400	16°	400	15(>7)	100	1.3(<1.7)	100
	CQX 48 A	25°	400	1-3	50	1.2(<1.7)	50
	CQX 48 B			4(>2.0)			
	TSSS 2600	25°	400	1.5(>0.6)	50	1.2(<1.6)	50
	TSUS 5200	15°	400	20(>10)	100	1.3(<1.7)	100
	TSUS 5201			25(>15)			
	TSUS 5202			30(>20)			
	TSUS 5400	22°	400	14(>7)	100	1.3(<1.7)	100
	TSUS 5401			17(>10)			
	TSUS 5402			20(>15)			

#### IR emitter GaAlAs (875 nm) in plastic package

	TSHA 4400	20°	300	20(>12)	100	1.5(<1.8)	100
	TSHA 4401			30(>16)			
	TSSA 2500	25°	300	10(>3.5)	100	1.5(<1.8)	100
	TSSA 4500	20°	300	23	100	1.5(<1.8)	100
	TSHA 5200	12°	300	40(>25)	100	1.5(<1.8)	100
	TSHA 5201			50(>30)			
	TSHA 5202			60(>36)			
	TSHA 5203			65(>50)			
	TSHA 5500	24°	300	20(>12)	100	1.5(<1.8)	100
	TSHA 5501			25(>16)			
	TSHA 5502			30(>20)			
	TSHA 5503			35(>24)			
	TSHA 6200	12°	300	40(>25)	100	1.5(<1.8)	100
	TSHA 6201			50(>30)			
	TSHA 6202			60(>36)			
	TSHA 6203			65(>50)			
	TSHA 6500	24°	300	20(>12)	100	1.5(<1.8)	100
	TSHA 6501			25(>16)			
	TSHA 6502			30(>20)			
	TSHA 6503			35(>24)			
	TSCA 6000	4°	300	120(>70)	100	1.5(<1.8)	100

Package	Type	Characteristics					
		+/- φ	t <sub>r</sub> , t <sub>f</sub> / ns	I <sub>e</sub> / mW/sr @ I <sub>F</sub> / mA	V <sub>F</sub> / V @ I <sub>F</sub> / mA		

### IR emitter GaAlAs/GaAs (950 nm) in plastic package

	TSIP 4400	20°	500	25(>12)	100	1.3(<1.8)	100
	TSIP 4401			30(>16)			
	TSSP 4400	20°	500	23(>10)	100	1.3(<1.8)	100
	TSIP 5200	17°	500	40(>20)	100	1.3(<1.8)	100
	TSIP 5201			50(>30)			
	TSIP 7600	30°	500	15(>8)	100	1.3(<1.8)	100
TSIP 7601	20(>12)						

### IR emitter GaAlAs/GaAs (950 nm) in SMD package

	TSML 3700	60°	500	7	100	1.3	100
--	-----------	-----	-----	---	-----	-----	-----

### IR emitter GaAs (950 nm) in SMD package

	TSMS 3700	60°	400	4	100	1.3(<1.7)	100
	TSMS 2100	60°	400	1	50	1.2(<1.7)	50

### IR emitter GaAs (950 nm) in hermetically sealed package

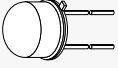
	TSTS 7100	5°	400	25(>10)	100	1.4(<1.7)	100
	TSTS 7101			12–25			
	TSTS 7102			20–40			
	TSTS 7103			32–64			
	TSTS 7300	12°	400	15(>4.0)	100	1.4(<1.7)	100
	TSTS 7301			6.3–12.5			
	TSTS 7302			10–20			
	TSTS 7303			16–32			
	TSTS 7500	40°	400	3(>1.2)	100	1.4(<1.7)	100
	TSTS 7501			1.6–3.2			
	TSTS 7502			2.5–5.0			
	TSTS 7503			4.0–8.0			

### IR emitter GaAlAs (875 nm) in hermetically sealed package

	TSTA 7100	5°	500	30(>20)	100	1.4(<1.8)	100
	TSTA 7300	12°		15(>10)			
	TSTA 7500	40°		6(>3.2)			

Package	Type	Characteristics					
		+/- φ	t <sub>r</sub> , t <sub>f</sub> / ns	I <sub>e</sub> / mW/sr @ I <sub>F</sub> / mA	V <sub>F</sub> / V @ I <sub>F</sub> / mA		

### IR emitter GaAs (950 nm) with metal socket and plastic lens

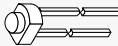
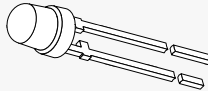
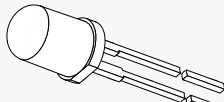

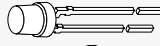

	CQX 19	20°	700	40	250	1.2	250
---	--------	-----	-----	----	-----	-----	-----

## 1.3 Detectors

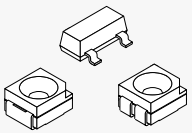
### Phototransistors

Package	Type	Photo Sensitive Area mm <sup>2</sup>	+/- φ	Characteristics			
				I <sub>ca</sub> / mA @ E <sub>e</sub> / mW / cm <sup>2</sup> (VCE = 5 V, λ = 950 nm)	t <sub>r</sub> / μs @ R <sub>L</sub> / kΩ (I <sub>C</sub> = 5 mA, λ = 950 nm)		

### Phototransistors in clear plastic package

	BPW 16 N	0.36	40°	0.14(>0.07)	1	3.7	0.1
	BPW 17 N		12.5°	1.0(>0.5)			
	BPW 85 A	0.18	25°	0.8–2.5	1	1.5	0.1
	BPW 85 B			1.5–4.0			
	BPW 85 C			3.0–8.0			
	BPW 96 A	0.18	20°	1.5–4.5	1	1.5	0.1
	BPW 96 B			2.5–7.5			
	BPW 96 C			4.5–15			
	BPV 11	0.36	15°	10(>3)	1	3.8	0.1
	S 351 P		20°	>4			
	TEPT 4700	0.36	60°	0.7–2.1	1	3.8	0.1
	TEYT 5500	0.18		0.6(>0.4)	1	1.5	0.1

### SMD Phototransistors in clear plastic package

	TEMT 2100	0.18	70°	0.45(>0.3)	1	1.5	0.1
	TEMT 2200*			0.45(>0.3)			
	TEMT 3700	0.07	70°	0.5(>0.2)	1	5	1
	TEMT 4700*			0.5(>0.2)			

\* with base connected



Package	Type	Photo Sensitive Area mm <sup>2</sup>	+/- φ	Characteristics			
				I <sub>ca</sub> / mA @ E <sub>e</sub> / mW / cm <sup>2</sup> (VCE = 5 V, λ = 950 nm)	t <sub>r</sub> / μs @ R <sub>L</sub> / kΩ (I <sub>C</sub> = 5 mA, λ = 950 nm)		

### Phototransistors in plastic package with filter matched for GaAs IREDs (950 nm)

	S 350 P	0.36	40°	1(>0.2)	1	3.8	0.1
	BPW 78 A	0.36	25°	1.0-3.0	1	3.8	0.1
	BPW 78 B		25°	4(>2.0)			
	TEFT 4300	0.18	30°	3.2(>0.8)	1	1.5	0.1
	TEST 2500*	0.36	35°	6(>3.0)	1	3.8	0.1
	TEST 2600	0.36	30°/60°	2.5(>1.0)	1	3.8	0.1
	BPV 11 F	0.36	15°	9(>3.0)	1	3.8	0.1

\* filter matched for GaAlAs IREDs

### Photodarlington in plastic package with filter matched for GaAs IREDs (950 nm)

	S 289 P	0.21	30°	15(>4.0)	0.3	80	0.1
--	---------	------	-----	----------	-----	----	-----

### Phototransistors in hermetically sealed package

	BPW 76 A	0.36	40°	0.4-0.6	1	3.8	0.1
	BPW 76 B			1.2(>0.6)			
	BPX 38	0.76	40°	>0.5	0.5	15	1
	BPX 38-4			0.5-1.0			
	BPX 38-5			0.8-1.6			
	BPX 38-6			>1.25			
	BPW 77 NA	0.36	10°	7.5-15	1	3.8	0.1
	BPW 77 NB			20(>10.0)			
	S 254 PN	0.18		>3.0		1.5	
	BPX 43	0.76	15°	>2.0	0.5	15	1
	BPX 43-4			2.0-4.0			
	BPX 43-5			3.2-6.3			
	BPX 43-6			>5.0			

### Photodarlington transistor in hermetically sealed package

	BPX 99 R-2	0.21	12.5°	10(>4.0)	0.3	80	0.1
	BPX 99 R-3			20(>10.0)			

## PIN photodiodes

Package	Type	Photo Sensitive Area mm <sup>2</sup>	+/- φ	Characteristics		
				I <sub>ra</sub> / μA (E <sub>e</sub> = 1 mW/cm <sup>2</sup> )	@ λ / nm	t <sub>on</sub> /ns (λ = 820 nm)

### PIN photodiodes in clear plastic package

	BPW 34	7.5	65°	50(>40)	950	100	1000
	BPW 46	7.5	65°	50(>40)	950	100	1000
	BPW 43	0.25	25°	8(>4)	950	4 <sup>1)</sup>	50
	BPV 10	0.78	17,5°	65(>38)	950	2.5 <sup>2)</sup>	50
	S 268 P	3x7.5	65°	50(>40)	950	100	1000
	TEMD 2100	0.25	75°	2.3	950	2.5 <sup>1)2)</sup>	50

### PIN photodiodes in plastic package with filter matched for GaAlAs IREDs (875 nm)

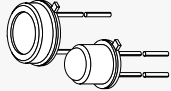
	BPW 82 *	7.5	65°	48(>41)	870	100	1000
	BPW 83 *	7.5	65°	50(>41)	870	100	1000
	BPV 20 NFL	7.5	65°	60(>40)	870	100	1000
	BPV 22 NF	7.5	60°	85(>55)	870	100	1000
	BPV 23 NF *	5.7	60°	65(>45)	870	70	1000
	BPV 23 NFL	5.7	60°	65(>45)	870	100	1000

### PIN photodiodes in plastic package with filter matched for GaAs IREDs (950 nm)

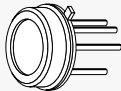
	BP 104	7.5	65°	45(>40)	950	100	1000
	BPW 41 N *	7.5	65°	45(>41)	950	100	1000
	S 186 P *	7.5	65°	45(>41)	950	100	1000
	BPV 20 F *	7.5	65°	60(>40)	950	100	1000
	BPV 21 F *	5.7	65°	38(>27)	950	70	1000
	BPV 22 F *	7.5	60°	80(>55)	950	100	1000
	BPV 23 F *	5.7	60°	63(>45)	950	70	1000
	BPV 10 F	0.78	17.5°	60(>30)	950	2.5 <sup>1)2)</sup>	50

Package	Type	Photo Sensitive Area mm <sup>2</sup>	+/- φ	Characteristics			
				I <sub>ra</sub> / μA @ λ / nm (E <sub>e</sub> = 1 mW/cm <sup>2</sup> )	t <sub>on</sub> /ns @ R <sub>L</sub> / Ω (λ = 820 nm)		

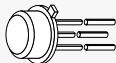
### PIN photodiodes in hermetically sealed package for standard applications

	S 153 P	7.5	50°	50(>40)	950	100	1000
	BPW 24 R	0.78	12°	65(>45)	950	7 <sup>1)3)</sup>	50

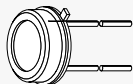
### Quadrant photodetector

	S 239 P	4 × 2.25	50°	15 (> 10)	870	150	1000
---	---------	----------	-----	-----------	-----	-----	------

### PIN photodiode in hermetically sealed package for glass fiber applications (Anode and cathode insulated from case)

	BPW 97	0.25	55°	1.3 (> 1)	870	0.6	50
---	--------	------	-----	-----------	-----	-----	----

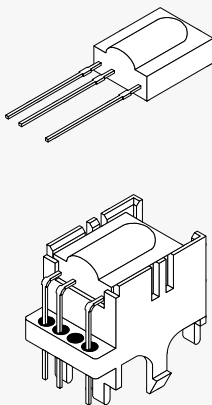
### Photodiodes for light measurement applications

Package	Type	Photo Sensitive Area mm <sup>2</sup>	+/- φ	Characteristics			
				I <sub>k</sub> / μA @ V <sub>0</sub> / mV (E <sub>A</sub> = 1 klx)	t <sub>on</sub> / μs @ R <sub>L</sub> / kΩ (I <sub>ph</sub> = 100 μA)		
	BPW 20 R	7.5	50°	61(>20)	500	3.5 <sup>1)</sup>	1
	BPW 21 R (with V(λ)filter)	7.5	50°	9(>4.5)	450	3.5 <sup>1)</sup>	1

<sup>1)</sup> t<sub>r</sub>, t<sub>f</sub> <sup>2)</sup> V<sub>R</sub> = 50 V <sup>3)</sup> V<sub>R</sub> = 20 V \* long lead packages optional: suffix "L", e.g. BPV 23 NFL

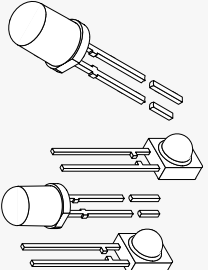
## 1.4 Photomodules

### Photomodules for pulse code remote control systems – standard applications

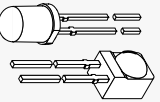
Package	Type	Characteristics					Features
		f <sub>0</sub> (kHz)	λ (nm)	V <sub>S</sub> (V)	E <sub>e</sub> min mW/m <sup>2</sup>		
	TFMS 5300	30	950	5	0.35	Photo detector and preamplifier in one package Reliable function even in disturbed ambient Internal protection against uncontrolled output pulses Internal shielding, daylight filter epoxy package High sensitivity and maximum interference safety against optical and electrical disturbances Output signal compatible to micro computers Maximum duty cycle of 40 %, minimum burst length 400 μs	
	TFMS 5330	33					
	TFMS 5360	36					
	TFMS 5380	38					
	TFMS 5400	40					
	TFMS 5560	56					
	TFMT 5300	30	950	5	0.35		
	TFMT 5330	33					
	TFMT 5360	36					
	TFMT 5380	38					
	TFMT 5400	40					
	TFMT 5560	56					

## 1.5 IrDA-infrared data transmission

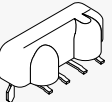
### Emitters

Package	Type	Characteristics					
		+/- φ	t <sub>r</sub> , t <sub>f</sub> / ns	I <sub>e</sub> / mW/sr	@ I <sub>F</sub> / mA	V <sub>F</sub> / V	@ I <sub>F</sub> / mA
	TSHA 5500	24°	300	20(>12)	100	1.5(<1.8)	100
	TSHA 5501			25(>16)			
	TSHA 5502			30(>20)			
	TSHA 5503			35(>24)			
	TSSA 4500	20°	300	23	100	1.5(<1.8)	100
	TSHF 5400	24°	30	30	100	1.35(<1.6)	100
	TSSF 4500	22°	30	20	100	1.35(<1.6)	100

### Detectors

Package	Type	Photo Sensitive Area mm <sup>2</sup>	+/- φ	Characteristics			
				I <sub>ra</sub> / μA	@ λ / nm	t <sub>on</sub> /ns	@ R <sub>L</sub> / Ω
	BPV 10 NF	0.78	20°	55	870	2.5	50
	BPV 22 NF	7.5	60°	85(>55)	870	100	1000
	BPV 23 NF	5.7	60°	65(>45)	870	70	1000

### Transceivers

Package	Type	+/- φ	V <sub>S</sub> / V	d <sub>min</sub> / m	t <sub>r</sub> , t <sub>f</sub> / ns	Data Rate / kBit/s	
						Min	Max
	TFDS 3000 <sup>*)</sup>	20°	5	1	< 200	2.4	115.2

\*) Production series of Integrated Transceiver starts in March '95. IrDA Evaluation Kits (discrete assembly on PCB with same function) are available.

## 2. Explanation of technical data

### 2.1 Type designation code for semiconductor devices according to Pro Electron

The type number of semiconductor devices consists of:

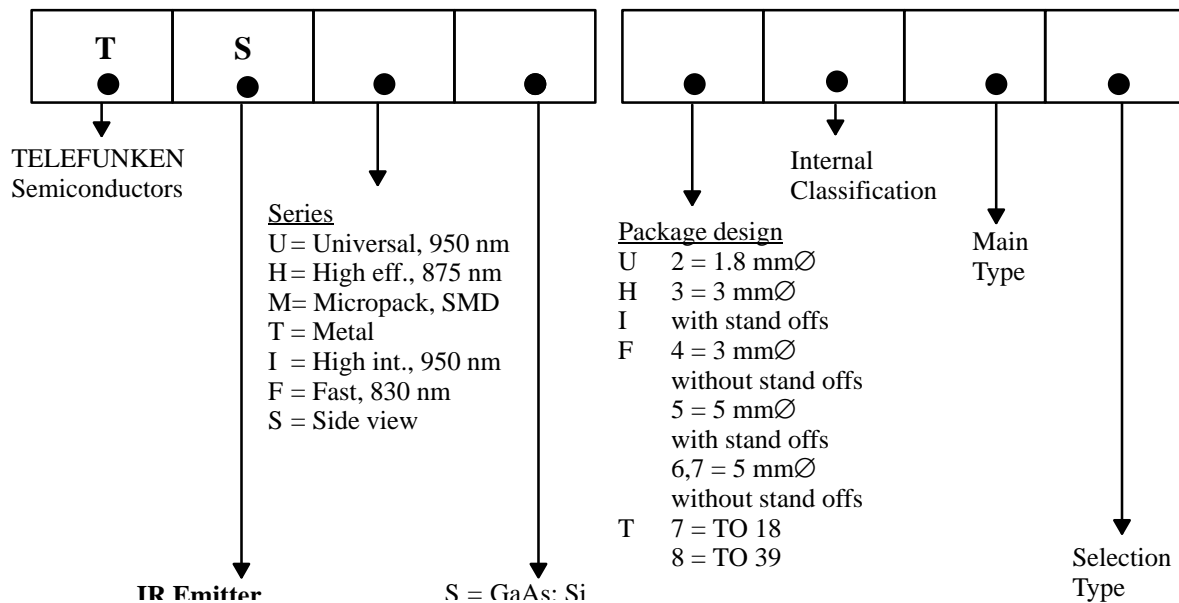
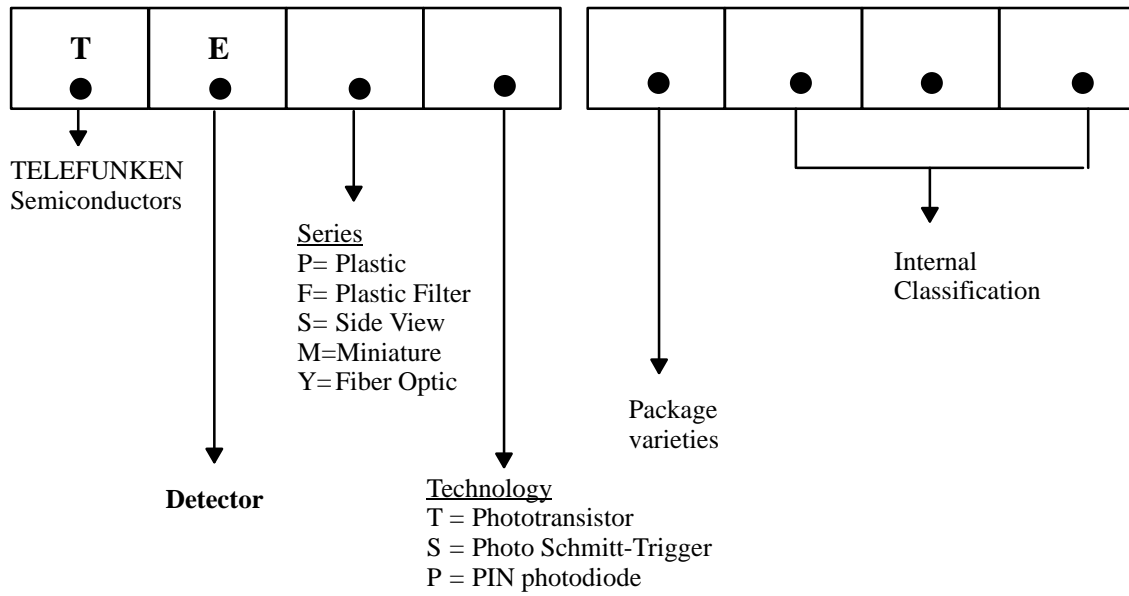
Two letters followed by a serial number

For example:

	B	P	W20	
	└───┬───┬───┘			
	Material	Function	Serial number	
The <b>first letter</b> gives information about the material used for the active part of the devices.	frequency			U TRANSISTOR: Power, switching
A GERMANIUM (Materials with a bandgap 0.6–1.0 eV) <sup>1)</sup>	E DIODE: Tunnel			X DIODE: Multiplier, e.g. varactor, step recovery
B SILICON (Materials with a bandgap 1.0–1.3 eV) <sup>1)</sup>	F TRANSISTOR: Low power, high frequency			Y DIODE: Rectifying, booster
C GALLIUM-ARSENIDE (Materials with a bandgap > 1.3 eV) <sup>1)</sup>	G DIODE: Miscellaneous	Oscillator,		Z DIODE: Voltage reference or transient suppressor diode
R COMPOUND MATERIALS (For instance Cadmium-Sulphide)	H DIODE: Magnetic sensitive			The <b>serial number</b> consists of:
The <b>second letter</b> indicates the circuit function:	K HALL EFFECT DEVICE: in an open magnetic circuit			<ul style="list-style-type: none"> <li>● Three figures, running from 100 to 999, for devices primarily intended for consumer equipment.</li> <li>● One letter (Z, Y, X, etc.) and two figures running from 10 to 99, for devices primarily intended for professional equipment.</li> </ul>
A DIODE: Detection, switching, mixer	L TRANSISTOR: Power, high frequency			A version letter can be used to indicate a deviation of a single characteristic, either electrically or mechanically. The letter never has a fixed meaning, the only exception being the letter R, indicating reversed voltage, i.e. collector to case.
B DIODE: Variable capacitance	M HALL EFFECT DEVICE: in a closed magnetic circuit			
C TRANSISTOR: Low power, audio frequency	N PHOTO COUPLER			
D TRANSISTOR: Power, audio	P DIODE: Radiation sensitive			
	Q DIODE: Radiation generating			
	R THYRISTOR: Low power			
	S TRANSISTOR: Low power, switching			
	T THYRISTOR: Power			

<sup>1)</sup> The materials mentioned are examples

## 2.2 TEMIC Type designation systems



## 3. Data sheet illustration

### 3.1 Symbols and terminology

A	and	Candela	on an element of the surface containing the point, by the area of that element
Anode, anode terminal		SI unit of luminous intensity $I_v$	
A		$C_D$	
Radiant sensitive area		Diode capacitance	$E_e = \frac{d\Phi_e}{dA}$
That area which is radiant sensitive for a specified range.		Total capacitance effective between the diode terminals due to case, junction and parasitic capacitances.	$E_e$ "ON" Irradiance for threshold "ON" Unit: $W/m^2$ or $mW/cm^2$
a		$C_j$	
Distance between the emitter (source) and the detector.		Junction capacitance	$E_v$
		Capacitance due to a pn junction of a diode.	Illuminance (at a point of a surface)
		It decreases with increasing reverse voltage.	Quotient of the luminous flux incident on an element of the surface containing the point, by the area of that element.
AQL		E	
Acceptable Quality Level		Emitter, emitter terminal (phototransistor)	$E_v = \frac{d\Phi_v}{dA}$
B		$E_A$	Unit: lx (Lux) = $lm/m^2$
Base, base terminal		Illumination at standard illuminant A	
C		According to DIN 5033 and IEC 306-1, illumination emitted from a tungsten filament lamp with a color temperature $T_f = 2855.6$ K which is equivalent to standard illuminant A.	f
Capacitance		Unit: lx (Lux) or klx.	Frequency
C			Unit: Hz (Hertz)
Cathode, cathode terminal		$E_{A\text{ amb}}$	$f_c$
Collector, collector terminal		Ambient illumination at standard illuminant A	Cut-off frequency – detector devices
$^{\circ}C$		$E_{A(TO)}$	The frequency at which the incident radiation generates a photocurrent or a photovoltage of the 0.707 times the value of radiation at $f = 1$ kHz.
Centigrade resp. degree Celsius		Switch-on illuminance (standard illuminant A) of a photo threshold switch.	$f_s$
Unit of the centigrade scale; can also be used (beside K) to express temperature changes.			Switching frequency
Symbols: T, $\Delta T$		$E_{A(TU)}$	
$T (^{\circ}C) = T (K) - 273$		Switch-off illuminance	$G_B$
$C_{CEO}$		$E_e$	Gain bandwidth product
Collector-emitter capacitance		Irradiance (at a point of a surface)	Gain bandwidth product is defined as the product of M times the frequency of measurement, when the diode is biased for maximum obtainable gain (avalanche photodiode).
Capacitance between the collector and the emitter with open base.		Quotient of the radiant power incident	
cd			

H Hysteresis	Radiant intensity $I_e$ of emitters is typically measured with an angle $\leq 0.01$ sr on mechanical axis or off-axis in the maximum of the irradiation pattern.	$I_{ra}$ Reverse light current
$H = 100 (E_{eON} - E_{eOFF})/E_{eON} (\%)$		Reverse current under irradiation (IEC747-5)
$I_a$ Light current	$I_e = \frac{d\Phi_e}{d\Omega}$	Reverse light current which flows due to a specified irradiation/illumination in a photo electric device.
General: Current which flows through a device due to irradiation/illumination.	Unit: W/sr, mW/sr	$I_{ra} = I_{ro} + I_{ph}$
$I_B$ Base current	$I_F$ Continuous forward current	$I_{ro}$ Reverse dark current
$I_{BM}$ Base peak current	The current flowing through the diode in the direction of lower resistance.	Dark current (IEC747-5)
$I_C$ Collector current	$I_{FAV}$ Average (mean) forward current	Reverse current flowing through a photo electric device in the absence of irradiation.
$I_{ca}$ Collector light current	$I_{FM}$ Peak forward current	$I_{SB}$ Quiescent current
Collector current under irradiation (IEC747-5)	$I_{FSM}$ Surge forward current	$I_{SD}$ Supply current in dark ambient
Collector current which flows at a specified illumination/irradiation.	$I_k$ Short circuit current	$I_{SH}$ Supply current in bright ambient
$I_{CEO}$ Collector dark current, with open base	That value of the current which flows when a photovoltaic cell or a photodiode is short circuited ( $R_L \ll R_i$ ) at its terminals.	$I_v$ Luminous intensity (of a source in a given direction)
Collector emitter dark current (IEC747-5)	$I_{ph}$ Photocurrent (photo electric current)	Quotient of the luminous flux leaving the source propagated in an element of solid angle containing the given direction by the element of solid angle.
For radiant sensitive devices with open base and without illumination/radiation ( $E = 0$ ).	That part of the electric current in a photo electric detector which is produced by the photo electric effect.	Luminous intensity $I_e$ of emitters is typically measured with an angle $\leq 0.01$ sr on mechanical axis or off-axis in the maximum of the irradiation pattern.
$I_{CM}$ Repetitive peak collector current	$I_o$ dc output current	$I_v = \frac{d\Phi_v}{d\Omega}$
$I_e$ Radiant intensity (of a source in a given direction)	$I_R$ Reverse current, leakage current	Unit: cd (candela), lm/sr
Quotient of the radiant power leaving the source propagated in an element of solid angle containing the given direction, by the element of solid angle.	Current which flows when reverse bias is applied to a semiconductor junction.	$I_{v av}$ Luminous intensity, average



# TEMIC

## TELEFUNKEN Semiconductors

---

K

Kelvin

The SI unit of temperature T (also called the Kelvin temperature); can also be used for temperature differences (formerly °K).

$L_e$

Radiance (in a given direction, at a point on the surface of a source or a detector, or at a point on the part of a beam)

Quotient of the radiant flux leaving, arriving at, or passing through an element of surface at this point and propagated in directions defined by an elementary cone containing the given direction, by the product of the solid angle of the cone and the area of the orthogonal projection of the element of surface on a plane perpendicular to the given direction.

$$L_e = \frac{d^2 \Phi_e}{d\Omega dA \cos \theta}$$

$$\text{Unit: } \frac{\text{W}}{\text{sr m}^2} \text{ or } \frac{\text{mW}}{\text{sr cm}^2}$$

lm

Lumen

Luminous flux,  $\Phi_v$

$L_v$

Luminance (in a given direction, at a point on the surface of a source or a receptor, or at a point on the path of a beam). Quotient of the luminous flux leaving, arriving at, or passing through an element of surface at this point and propagated in directions defined by an elementary cone containing the given direction, by the product of the solid angle of the cone and the area of the orthogonal projection of the element of source on

a plane perpendicular to the given direction.

$$L_v = \frac{d^2 \Phi_v}{d\Omega dA \cos \theta}$$

Unit:  $\text{cd/m}^2$

lx

Lux

M

The voltage dependent photocurrent gain M is defined as the ratio of photocurrent  $I_{ph}$  at a certain reverse voltage to the photocurrent at a bias of 10 V (avalanche photodiode).

m

Matching factor

Emitter arrays:

The ratio of the minimum to the maximum radiant intensity value measured on the devices constituting an array.

Detector arrays:

The ratio of the minimum to the maximum light current of the devices constituting an array.

$M_e$

Radiant exitance (at a point of a surface)

Quotient of the radiant flux leaving an element of the surface containing the point, by the area of that element.

$$M_e = \frac{d\Phi_e}{dA}$$

Unit:  $\text{W/m}^2$

$M_v$

Luminous emittance (at a point of a surface)

Quotient of the luminous flux leaving an element of the surface containing the point, by the area of that element.

$$M_v = \frac{d\Phi_v}{dA}$$

Unit:  $\text{lm/m}^2$

N.A.

Numerical Aperture

N.A. =  $\sin \alpha/2$

This term is used for the characteristic of sensitivity or intensity angles of fiber optics and objectives.

NEP

Noise Equivalent Power

$P_{tot}$

Total power dissipation

$P_v$

Power dissipation, general

$Q_e$

Radiant energy

Energy emitted, transferred or received in the form of radiation.

$$Q_e = \int \Phi_e \times dt$$

Unit: J (Joule), Ws

$Q_v$

Luminous energy of light

Product of luminous flux and its duration.

$$Q_v = \int \Phi_v \times dt$$

Unit:  $\text{lm s}$  (lumen second)

$R_D$

Dark resistance

$R_F$

Feedback resistor

$R_H$

Resistor for programming the hysteresis of a photo threshold switch.

$R_i$

Internal resistance

<p><math>R_{is}</math> Isolation resistance</p> <p><math>R_L</math> Load resistance</p> <p><math>R_S</math> Serial resistance</p> <p><math>R_{sh}</math> Shunt resistance is defined and measured at a voltage of 10 mV forward or reverse, or peak to peak</p> <p><math>R_{(TO)}</math> Resistor for programming the threshold of a photo threshold switch</p> <p><math>R_{thJA}</math> Thermal resistance, junction to ambient</p> <p><math>R_{thJC}</math> Thermal resistance, junction to case</p> <p><math>S</math> Sensitivity, absolute Ratio of the output value Y of a radiant sensitive device to input value X of a physical quantity: <math display="block">S = \frac{Y}{X}</math> Unit: A/lx, A/W</p> <p><math>S_{(TH)}</math> Threshold sensitivity</p> <p><math>s(\lambda)</math> Absolute spectral sensitivity, at a wavelength <math>\lambda</math> The ratio of the output quantity to the radiant input quantity in the range of wavelengths <math>\lambda</math> to <math>(\lambda + d\lambda)</math>: <math display="block">s(\lambda) = \frac{dy(\lambda)}{dx(\lambda)}</math></p>	<p>e.g. the radiation power <math>\Phi_{e(\lambda)}</math> at a specified wavelength <math>\lambda</math> is falling on the radiation sensitive area of a detector, which generates a photocurrent <math>I_{ph}</math>. <math>s(\lambda)</math> is the ratio between the generated photocurrent <math>I_{ph}</math> and the radiation power <math>\Phi_{e(\lambda)}</math> falling on the detector. <math display="block">s(\lambda) = \frac{I_{ph}}{\Phi_{e(\lambda)}}</math> Unit: <math>\frac{A}{W}</math> or <math>\frac{mA}{mW}</math></p> <p><math>s(\lambda)_{rel}</math> Spectral sensitivity, relative Ratio of the radiant sensitivity at any considered wavelength <math>s(\lambda)</math> to the radiant sensitivity <math>s(\lambda_0)</math> at a certain wavelength <math>\lambda_0</math> taken as a reference. <math display="block">s(\lambda)_{rel} = \frac{s(\lambda)}{s(\lambda_0)}</math></p> <p><math>s(\lambda_0)</math> Spectral sensitivity at reference wavelength <math>\lambda_0</math></p> <p><math>s(\lambda_p)</math> Spectral sensitivity at wavelength <math>\lambda_p</math></p> <p>sr Steradian Unit of solid angle <math>\Omega</math></p> <p>T Period (duration)</p> <p>T Temperature 0 K = -273.16°C Unit: K (Kelvin), °C (Centigrade/degree Celsius)</p> <p>t Time</p>	<p><math>t_{pi}</math> Input pulse duration</p> <p><math>t_{po}</math> Output pulse duration</p> <p><math>T_{amb}</math> Ambient temperature If self-heating is significant: Temperature of the surrounding air below the device, under conditions of thermal equilibrium. If self-heating is insignificant: Air temperature in the surroundings of the device.</p> <p><math>T_{amb}</math> Ambient temperature range As an absolute maximum rating: The maximum permissible ambient temperature range.</p> <p><math>T_C</math> Temperature coefficient The ratio of the relative change of an electrical quantity to the change in temperature (<math>\Delta T</math>) which causes it, under otherwise constant operating conditions.</p> <p><math>T_{case}</math> Case temperature The temperature measured at a specified point on the case of a semiconductor device. Unless otherwise stated, this temperature is given as the temperature of the mounting base for devices with metal can.</p> <p><math>t_d</math> Delay time</p>
--	--	--

$T_f$   
color temperature  
Temperature of the thermal radiator which emits radiation of the same chromaticity as the radiation considered.

Unit: K (Kelvin).

$t_f$   
Fall time

$T_j$   
Junction temperature  
The spatial mean value of temperature during operation. In case of phototransistors, it is mainly the temperature of collector junction because its inherent temperature is maximum.

$t_{off}$   
Turn-off time

$t_{on}$   
Turn-on time

$t_p$   
Pulse duration

$t_r$   
Rise time

$t_s$   
Storage time

$T_{sd}$   
Soldering temperature  
Maximum allowable temperature for soldering with specified distance from case and its duration.

$T_{stg}$   
Storage temperature range  
The temperature range at which the device may be stored or transported without any applied voltage.

$V_{BEO}$   
Base emitter voltage, open collector

$V_{(BR)}$   
Breakdown voltage  
Reverse voltage at which a small increase in voltage results in a sharp rise of reverse current. It is given in technical data sheet for a specified current.

$V_{(BR)CEO}$   
Collector emitter breakdown voltage, open base

$V_{(BR)EBO}$   
Emitter base breakdown voltage, open collector

$V_{(BR)ECO}$   
Emitter collector breakdown voltage, open base

$V_{CBO}$   
Collector base voltage, open emitter  
Generally reverse biasing is to apply a voltage to any of two terminals of a transistor in such a way that one of the junction operates in reverse direction, whereas the third terminal (second junction) is specified separately.

$V_{CE}$   
Collector emitter voltage

$V_{CEO}$   
Collector emitter voltage, open base ( $I_B = 0$ )

$V_{CEsat}$   
Collector emitter saturation voltage  
Saturation voltage is the dc voltage between collector and emitter for specified (saturation) conditions i.e.  $I_C$  and  $E_V$  ( $E_c$  or  $I_B$ ) whereas the

operating point is within the saturation region.

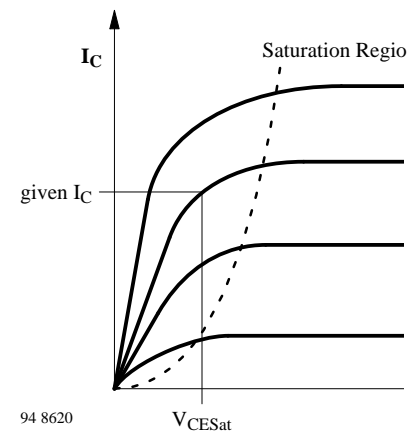


Figure. 3.1

$V_{EBO}$   
Emitter base voltage, open collector

$V_{ECO}$   
Emitter collector voltage, open base

$V_F$   
Forward voltage  
The voltage across the diode terminals which results from the flow of current in the forward direction.

$V_{is}$   
Isolation voltage – opto isolator  
Maximum allowable operating voltage between input and output.

$V_O$   
Open circuit voltage  
Voltage measured between the photovoltaic cell or photodiode terminals at a specified radiation/illumination, if the circuit is open

$V_{OH}$ Output voltage high	$V_{ph}$ Photovoltage Voltage generated between the photovoltaic cell or photodiode terminals due to	radiation/illumination.
$V_{OL}$ Output voltage low		$V_O$ Output voltage
$V_{no}$ Signal to noise ration	Angle of half intensity	$\lambda_p$ Wavelength of peak sensitivity or emission
$V_R$ Reverse voltage Voltage drop which results from the flow of a reverse current.	$\varphi_{1/2}$ Angle of half transmission distance	$\Delta V_o$ Output voltage change (differential output voltage)
$V_S$ Supply voltage	$\lambda$ Wavelength, general The wavelength of an electromagnetic radiation.	$\Delta\lambda$ Spectral half bandwidth The wavelength interval within which the spectral sensitivity or spectral emission falls to half peak value.
$V(\lambda)$ Standard luminous efficiency function for photopic vision	$\lambda_{0.5}$ Range of spectral bandwidth (50 %) The range of wavelengths within which the spectral sensitivity or spectral emission remains within 50 % of the maximum value.	$\Phi_e$ Radiant flux, radiant power Power emitted, transferred, or received in form of radiation.
$\varphi = \alpha/2$ Angle of half sensitivity	$\lambda_D$ Dominant wavelength	
$\Phi_e = \frac{dQ_e}{dt}$		
Unit: W (Watt)	A quantity derived from the radiant flux by spectrally $V(\lambda)$ – weighting of the radiation spectrum multiplied by the photometric efficiency constant	$K_m = 683 \text{ lm/W}$ $\Phi_v = K_m * \int V(\lambda) * \Phi_e(\lambda) * d\lambda$
$\Phi_v$ Luminous flux $\Phi_v = \frac{dQ_v}{dt}$		
Unit: lm (lumen)		
$\eta$ Quantum Efficiency	The space enclosed by rays which emerge from a single point and lead to all the points of a closed curve. If it is assumed that the apex of the cone formed in this way is the center of a	sphere with radius r and that the cone intersects with the surface of the sphere, then the size of the surface area (A) of the sphere subtending the cone is a measure of the solid angle
$\Omega$ Solid angle, see figure 3.2 $\Omega = \frac{A}{r^2}$		
There are $4\pi$ sr in a complete sphere. A cone with an angle of half sensitivity $\alpha/2$ forms a solid angle of	$\Omega = 2\pi (1 - \cos \alpha/2) = 4\pi \sin^2 \alpha/4$ Unit: sr (Steradian)	

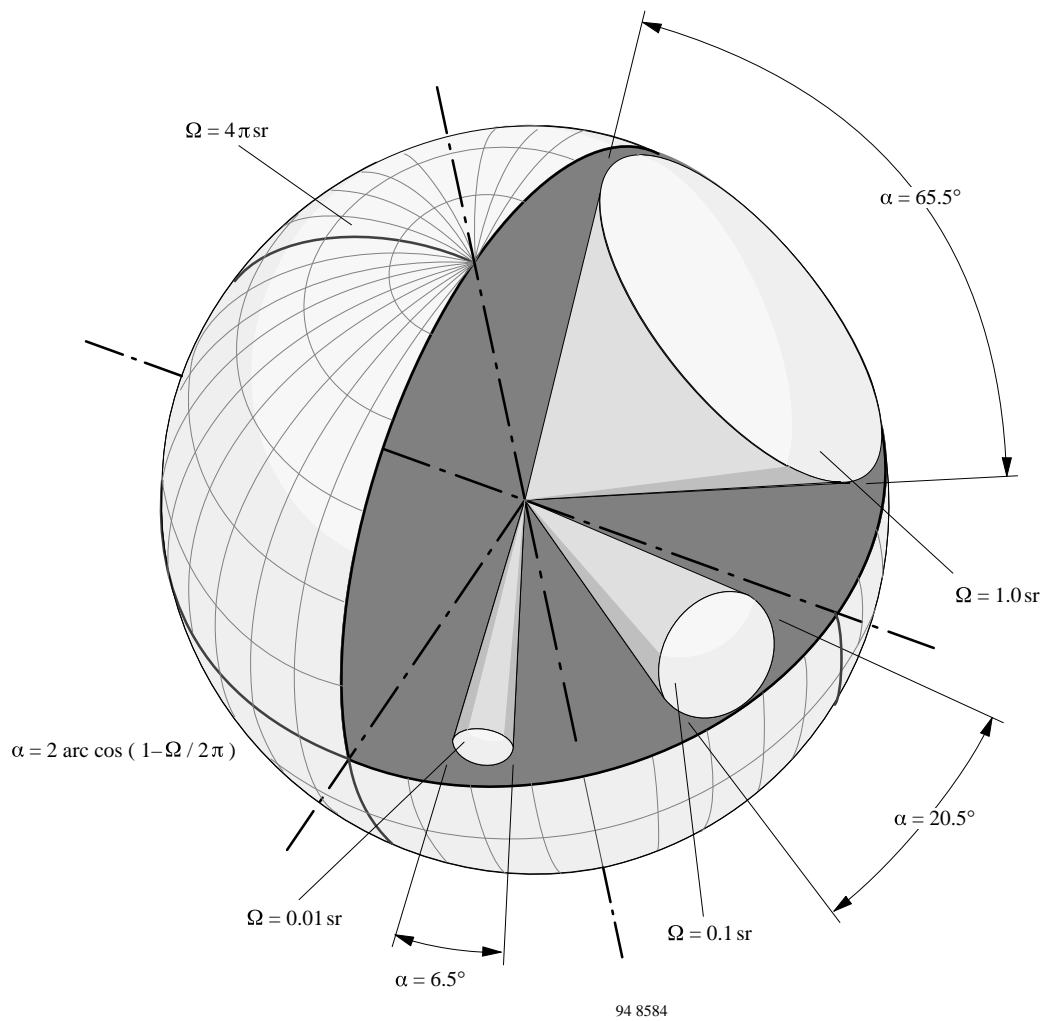


Figure 3.2

## Examples of the application of the symbols

according to 41785 and IEC 148

### a) Transistor

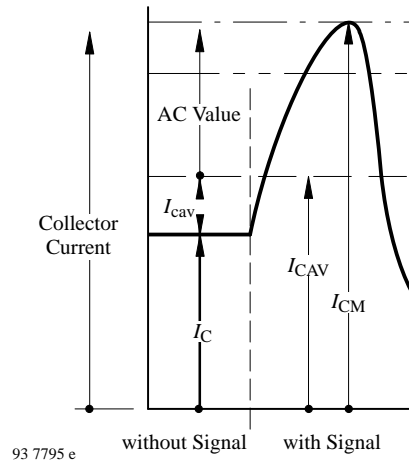


Figure 3.3

$I_C$	dc value, no signal
$I_{CAV}$	Average total value
$I_{CM}; I_C$	Maximum total value
$I_{CEFF}$	RMS total value
$I_C; I_{CEFF}$	RMS varying component
$I_{CM}; I_C$	Maximum varying component value
$i_C$	Instantaneous total value
$i_c$	Instantaneous varying component value

It is valid:

$$I_{CM} = I_{CAV} + I_{CM}$$

$$I_{CEFF} = \sqrt{I_{CAV}^2 + I_{ceff}^2}$$

$$i_C = I_{CAV} + i_c$$

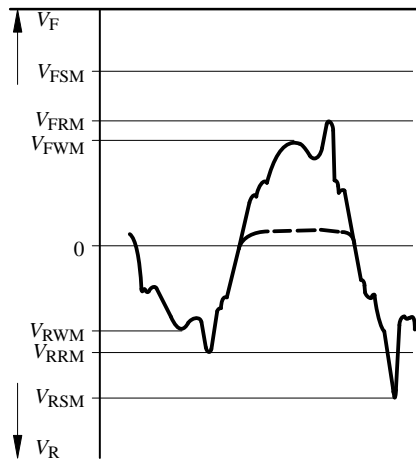


Figure 3.4

$V_F$	Forward voltage
$V_R$	Reverse voltage
$V_{FSM}$	Surge forward voltage (non-repetitive)
$V_{RSM}$	Surge reverse voltage (non-repetitive)
$V_{FRM}$	Repetitive peak forward voltage
$V_{RRM}$	Repetitive peak reverse voltage
$V_{FWM}$	Crest working forward voltage
$V_{RWM}$	Crest working reverse voltage

c) Designation and symbols of optoelectronic devices are given so far as possible, according to DIN 44020 sheet 1 and IEC publication 50(45).

## Terms of Radiometry and Photometry

Radiometric Units			Photometric Units			Note
Unit	Symbol	Unit	Unit	Symbol	Unit	
Radiant flux, Radiant power	$\Phi_e$	Watt, W	Luminous flux	$\Phi_v$	Lumen, lm	Power
Radiant exitance, Emittance	$M_e$	W/m <sup>2</sup>	Luminous emittance	$M_v$	lm/m <sup>2</sup>	Output power per unit area
(Radiant) intensity	$I_e$	W/sr	(Luminous) intensity	$I_v$	Candela, cd, lm/sr	Output power per unit solid angle
Radiant sterance, Radiance	$L_e$	$\frac{W}{sr \cdot m^2}$	Luminance (Brightness, sterance)	$L_v$	cd/m <sup>2</sup>	Output power per unit solid angle and emitting area
Radiant incidence, Irradiance	$E_e$	W/m <sup>2</sup>	Illuminance	$E_v$	lm/m <sup>2</sup> Lux, lx	Input power per unit area
Radiant energy	$Q_e$	Ws	Luminous energy	$Q_v$	lm s	Power * time
Irradiation	$H_e$	Ws/m <sup>2</sup>	Illumination	$H_v$	lm s/m <sup>2</sup>	Radiant energy or luminous energy per unit area

## 3.2 Data sheet construction

Data sheet information is generally presented in the following sequence:

- Device description
- Absolute maximum ratings
- Thermal data – Thermal resistances
- Optical and electrical characteristics
- Diagrams
- Dimensions (Mechanical data)

### 3.2.1 Device description

The following information is provided: Type number, semiconductor materials used, sequence of zones, technology used, device type and, if necessary construction.

Also, short-form information on special features and the typical applications is given.

### 3.2.2 Absolute maximum ratings

These define maximum permissible operational and environmental conditions. If any one of these conditions is exceeded, this could result in the destruction of the device.

Unless otherwise specified, an ambient temperature of  $25 \pm 3^\circ\text{C}$  is assumed for all absolute maximum ratings.

Most absolute ratings are static characteristics; if measured by a pulse method, then the associated measurement conditions are stated. Maximum ratings are absolute (i. e. not interdependent).

Any equipment incorporating semiconductor devices must be designed so that even under the most unfavorable operating conditions the specified maximum ratings of the devices used are never exceeded. These ratings could be exceeded because of changes in

- supply voltage, the properties of other components used in the equipment

- control settings
- load conditions
- drive level
- environmental conditions and the properties of the devices themselves (i.e. ageing).

### 3.2.3 Thermal data – thermal resistances

Some thermal data (e. g. junction temperature, storage temperature range, total power dissipation), because they impose a limit on the application range of the device, are given under the heading "Absolute maximum ratings".

The thermal resistance junction ambient ( $R_{thJA}$ ) quoted is that which would be measured without artificial cooling, i.e. under the worst conditions.

Temperature coefficients, on the other hand, are listed together with the associated parameters under "Optical and electrical characteristics".



### 3.2.4 Basic characteristics

Under this heading optical and electrical characteristics and switching characteristics are grouped as the most important operational characteristics (minimum, typical and maximum values) together with associated test conditions supplemented with curves, an AQL-value being quoted for particularly important parameters.

### 3.2.5 Family of curves

Besides the static (dc) and dynamic (ac) characteristics, family of curves are given for specified operating conditions. They show the typical interdependence of individual

characteristics.

### 3.2.6 Dimensions (Mechanical data)

It contains important dimensions, sequence of connection supplemented by a circuit diagram. Case outline drawings carry DIN-, JEDEC or commercial designations. Information on angle of sensitivity or intensity and weight completes the list of mechanical data.

Note especially:

If the dimensional information does not include any tolerances, then the following applies:

Lead length and mounting hole dimensions are minimum values.

Radiant sensitive or emitting area respectively being typical, all other dimensions are maximum.

Any device accessories must be ordered separately, quoting the order number.

### Preliminary specifications

This heading indicates that some information on the device concerned may be subject to slight changes.

### Not for new developments

This heading indicates that the device concerned should not be used in equipment under development, it is, however, available for present production.

## Luminance; terms, conversion factors

Unit	$\frac{\text{cd/m}^2}{\text{Lumen/sr m}^2}$	$\frac{\text{cd/ft}^2}{\text{Lumen/sr ft}^2}$	$\frac{\text{cd/in}^2}{\text{Lumen/sr in}^2}$	asb Apostilb	sb Stilb	L Lambert	fL Foot-lambert
cd/m <sup>2</sup>	1	9.29*10 <sup>-2</sup>	6.454*10 <sup>-4</sup>	$\pi$	10 <sup>-4</sup>	$\pi$ *10 <sup>-4</sup>	0.2919
cd/ft <sup>2</sup>	10.764	1	6.94*10 <sup>-3</sup>	33.82	1.076*10 <sup>-3</sup>	3.382*10 <sup>-3</sup>	$\pi$
cd/in <sup>2</sup>	1550	144	1	4869	0.155	0.4869	452.4
asb	1/ $\pi$	2.957*10 <sup>-2</sup>	2.054*10 <sup>-4</sup>	1	10 <sup>-4</sup> / $\pi$	10 <sup>-4</sup>	0.0929
sb	10 <sup>4</sup>	929	6.452	$\pi$ *10 <sup>4</sup>	1	$\pi$	2919
L	10 <sup>4</sup> / $\pi$	2.957*10 <sup>2</sup>	2.054	10 <sup>4</sup>	1/ $\pi$	1	929
fL	3.426	1/ $\pi$	2.211*10 <sup>-3</sup>	10.764	3.426*10 <sup>-4</sup>	1.0764*10 <sup>-3</sup>	1

## Illuminance; terms, conversion factors

Unit	Lux, lx (Lumen/m <sup>2</sup> )	lm/cm <sup>2</sup> Lumen/cm <sup>2</sup>	fc Footcandle
Lux, lx	1	10 <sup>-4</sup>	0.0929
lm/cm <sup>2</sup>	10 <sup>4</sup>	1	929
Footcandle, fc	10.764	10.764*10 <sup>-4</sup>	1

## 4. Physics and technology

### 4.1 Emitters

#### 4.1.1 Materials

Infrared emitting diodes (IREDs) can be fabricated from a range of different III-V compounds. Unlike the elemental semiconductor silicon, the compound III-V semiconductors consists of two different elements of group three (e.g., Al, Ga, In) and five (e.g., P, As) of the periodic table. The bandgap energies of these compounds vary between 0.18 eV and 3.4 eV. However, the IREDs considered here emit in the near infrared spectral range between 800 nm and 1000 nm, and, therefore, the selection of materials is limited to GaAs and the mixed crystal  $Ga_{1-X}Al_XAs$ ,  $0 \leq X < 0.8$ , made from the pure compounds GaAs and AlAs.

Infrared radiation is produced by radiative recombination of electrons and holes from the conduction and valence bands. The emitted photon energy, therefore, corresponds closely to the bandgap energy  $E_g$ . The emission wavelength can be calculated according to the formula  $\lambda = 1.240 \mu\text{m eV}/E_g$ . The internal efficiency depends on the band structure, the doping material and the doping level. Direct bandgap materials offer high efficiencies, because no photons are needed for recombination of electrons and holes. GaAs is a direct gap material and  $Ga_{1-X}Al_XAs$  is direct up to  $X = 0.44$ . The doping species Si provides the best efficiencies and shifts the emission wavelength below the bandgap energy into the infrared spectral range by about 50 nm typically.

Charge carriers are injected into the material via pn junctions. Junctions of high injection efficiency are readily formed in GaAs and  $Ga_{1-X}Al_XAs$ . P-type conductivity can be obtained with metals of valency two, such as Zn

and Mg, n-type conductivity with elements of valency six, such as S, Se and Te. However, silicon, of valency four, can occupy sites of III-valence and V-valence atoms, and, therefore, acts as donor and as acceptor. The conductivity type depends primarily on the material growth temperature. Therefore – by exact temperature control – pn junctions can be grown with the same doping species Si on both sides of the junction. Ge, on the other hand, has also a valency of four, but occupies group V sites at high temperatures i.e. p-type.

Only monocrystalline material is used for IRED production. In the mixed crystal system  $Ga_{1-X}Al_XAs$ ,  $0 \leq X < 0.8$ , the lattice constant varies only by about  $1.5 \cdot 10^{-3}$ . Therefore, monocrystalline layered structures of different  $Ga_{1-X}Al_XAs$  compositions can be produced with extremely high structural quality. These structures are useful because the bandgap can be shifted from 1.40 eV (GaAs) to values beyond 2.1 eV. In this way transparent windows and heterogeneous structures can be fabricated. Transparent windows are another suitable means to increase efficiency, and heterogeneous structures can provide shorter switching times and higher efficiency. Such structures are termed double heterostructures (DH) and consist normally of two layers that confine a layer with a much smaller bandgap.

The best production method for all materials needed is liquid phase epitaxy (LPE). This method uses Ga-solutions containing As, possibly Al, and the doping substance. The solution is saturated at high temperature, typically 900°C, and GaAs substrates are dipped into the liquid. The solubility of As and Al decreases with decreasing temperature. Therefore epitaxial layers can be grown by slow cooling

of the solution. Several layers differing in composition may be obtained using different solutions one after another, as needed e.g. for DHs.

In liquid phase epitaxial reactors, production quantities of up to 50 wafers with several layers can be handled.

#### 4.1.2 IRED chips and characteristics

At present the most popular IRED chip is made only from GaAs. The structure of the chip is displayed in figure 4.1a.

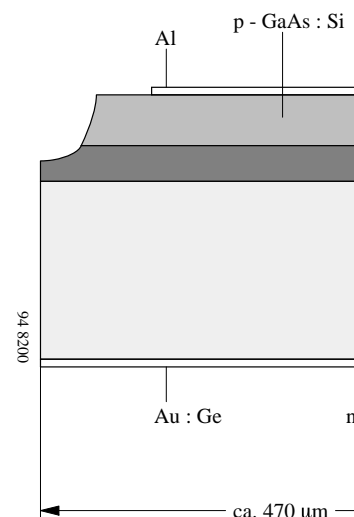


Figure 4.1a

On an n-type substrate, two Si-doped layers are grown by liquid phase epitaxy from the same solution. Growth starts as n-type at high temperature and becomes p-type below about 820°C. A structured Al-contact on the p-side and a large area Au:Ge contact on the back side provide a very low series resistance. The angular distribution of the emitted radiation is displayed in figure 4.1b.

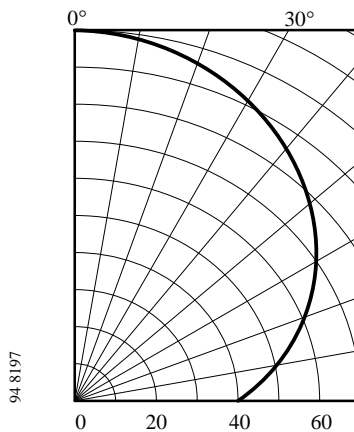


Figure 4.1b

The package of the chip has to provide a good collection efficiency of the radiation emitted sideways, and has to diminish the refractive index step between the chip ( $n = 3.6$ ) and the air ( $n = 1.0$ ) with an epoxy of refractive index 1.55. In this way the output power of the chip is increased by a factor of 3.5 for the assembled device.

The chip described is the most cost-efficient chip. The forward voltage at  $I_F = 1.5$  A has the lowest possible value. The total series resistance is typically only  $0.60 \Omega$ . The output power and the linearity (defined as the optical output power increase divided by the current increase between 0.1 and 1.5 A) are high. Relevant data on the chip and a typical assembled device are given in table 4.1.

The technology used for another chip eliminates the absorbing substrate and uses only a thick epitaxial layer. The chip is shown in figure 4.2a.

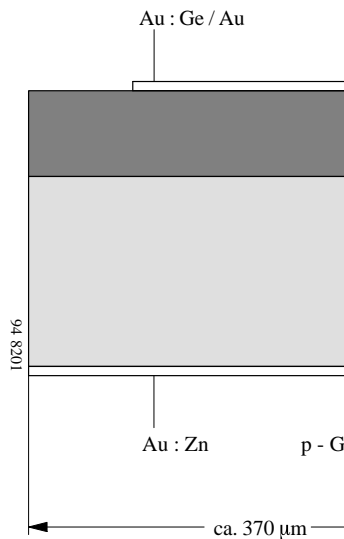


Figure 4.2a

Originally the GaAs substrate was adjacent to the n-side. Growth of  $Ga_{0.7}Al_{0.3}As$  started as n-type and became p-type – as in the first case – through the specific properties of the doping material Si. A characteristic feature of the Ga-Al-As phase system causes the Al-content of the growing epitaxial layer to decrease. Therefore the Al-concentration at the junction has dropped to 8% ( $Ga_{0.92}Al_{0.08}As$ ), producing an emission wavelength of 880 nm. During further growth the Al-content approaches zero. The gradient of the Al-content, and therefore, also of the bandgap energy, produces an emission band of a relatively large half width. The transparency of the large bandgap material results in a very high external efficiency on this type of chip.

The chip is mounted n-side up, and the front side metallization is Au:Ge/Au,

whereas the back side metallization is Au:Zn.

The angular distribution of the emitted radiation is displayed in figure 4.2b.

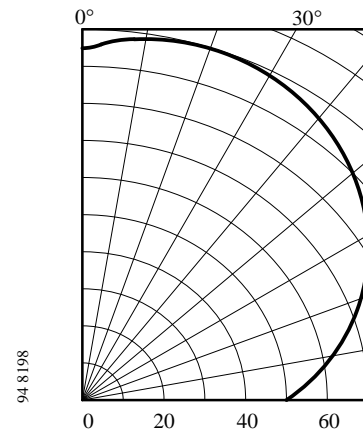


Figure 4.2b

The  $Ga_{1-x}Al_xAs$  chip described has one of the highest output powers of any chip available. Due to its shorter wavelength, the chip offers specific advantages in combination with a Si detector. Integrated Opto-ICs, like amplifiers or Schmitt Triggers, have higher sensitivities at shorter wavelengths. Similarly, phototransistors are also more sensitive. Finally the frequency bandwidth of pin diodes is higher at shorter wavelengths. Another important advantage of this chip is its high linearity up to and beyond 1.5 A. The forward voltage, however, is higher than the voltage of a GaAs chip. Table 4.1 provides more data on the chip.

A technology combining some of the advantages of the two technologies described above is summarized in figure 4.3a.

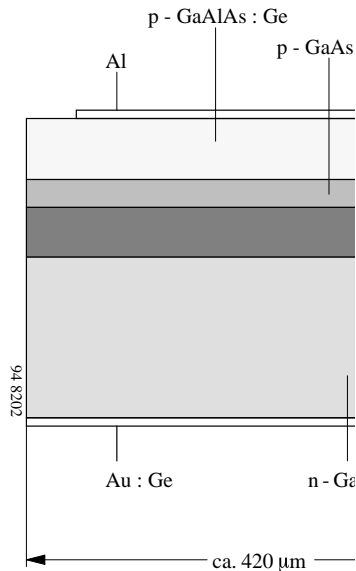


Figure 4.3a

Starting with the n-type substrate, n- and p-type GaAs layers are grown in a manner similar to the epitaxy of the standard GaAs:Si diode. After this, a highly transparent window layer of Ga<sub>1-x</sub>Al<sub>x</sub>As, doped p-type with Ge, is grown. The upper contact to the p-side is made of Al and the back side contact is Au:Ge. The angular distribution of the emitted radiation is shown in figure 4.3b.

Figure 4.3b

This chip type combines a relatively low forward voltage with a high electro-optical efficiency, offering an optimized combination between the advantageous characteristics of the two other chips. Refer again to table 4.1 for more details.

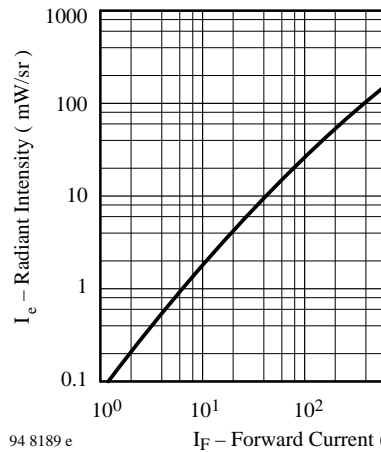


Table 4.1. Characteristic data of IRED chips

Technology	Typical chip data				Typical device	Typical device data				
	$\Phi_e$ /mW at 0.1 A	$\lambda_p$ /nm	$\Delta\lambda$ /nm	Polarity		$\Phi_e$ /mW at 0.1 A	$\Phi_e$ /mW at 1.5 A	$U_F$ /V at 0.1 A	$U_F$ /V at 1.5 A	$\Phi_e(1.5A)/\Phi_e(0.1A)$
GaAs on GaAs	4.3	950	50	p up	TSUS 540.	15	140	1.3	2.1	9
Ga <sub>1-x</sub> Al <sub>x</sub> As	6.7	875	80	n up	TSHA 550.	27	350	1.5	3.4	13
GaAs + Ga <sub>1-x</sub> Al <sub>x</sub> As on GaAs	5.8	950	50	p up	TSIP 520.	24	300	1.3	2.4	12

## 4.2 UV, visible, and near IR silicon photodetectors

(adapted from "Sensors, Vol 6, Optical Sensors, Chapt. 8, VCH – Verlag, Weinheim 1991)

### 4.2.1 Silicon photodiodes

#### 4.2.1.1 The physics of silicon detector diodes

The absorption of radiation is caused by the interaction of photons and the charge carriers inside a material. The different allowed energy levels and the band structure determine the likelihood of interaction and, therefore, the absorption characteristics of the semiconductors. The long wavelength cutoff of the absorption is given by the bandgap energy. The slope of the absorption curve depends on the physics of the interaction and is, for silicon, much weaker than for most other semiconducting materials. This results in the strongly wavelength-dependent penetration depth which is shown in figure 4.4. (The penetration depth is defined as that depth where 1/e of the incident radiation is absorbed.)

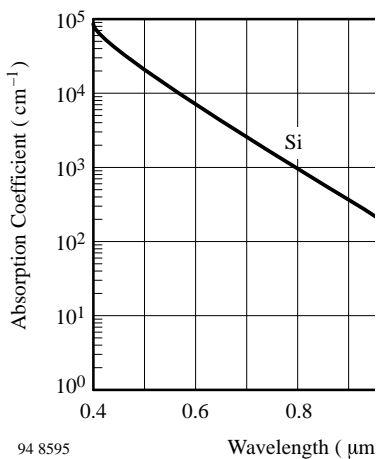


Figure 4.4. Absorption and penetration depth of optical radiation in silicon

Depending on the wavelength, the penetration depth varies from tenths of a micron at 400 nm (blue) to more than 100 μm at 1 μm (IR). For detectors to be effective, an interaction length of at least twice the penetration depth should be realized (equivalent to  $1/e^2 = 86\%$  absorbed radiation). In the pn diode, the generated carriers are collected by the electrical field of the pn junction. The effects in the vicinity of a pn junction are shown in figure 4.8 for various types and operating modes of the pn diode. The incident radiation generates mobile minority carriers—electrons in the p-side, holes in the n-side. In the short circuit mode shown in figure 4.5 (top), the carriers will drift under the field of the built-in potential of the pn junction. Other carriers diffuse inside the field-free region along a concentration gradient, resulting in an electrical current through the applied load, or without load, in an external voltage, resulting in the open circuit voltage  $V_{OC}$ , at the contact terminals. The bending of the energy bands near the surface is caused by surface states. An equilibrium is established between the generation, the recombination of carriers, and current flow through the load.

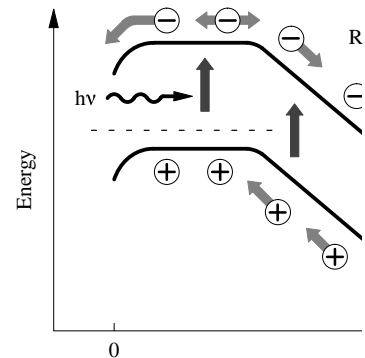
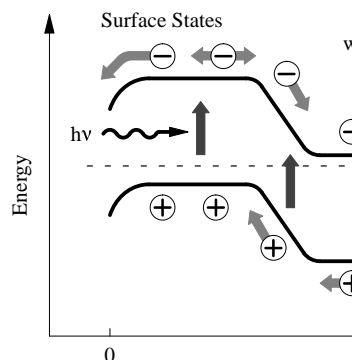


Figure 4.5. Generation-recombination effects in the vicinity of a pn junction. Top: Short circuit mode, bottom: reverse biased

The recombination takes place inside the bulk material with technology and process dependent time constants which are very small near the contacts and the surfaces of the device. For short wavelengths with very small penetration depths, the carrier recombination is the efficiency limiting process. To achieve high efficiencies, as many carriers as possible should be separated by the electrical field inside the space charge region. This is a very fast process, much faster than the typical recombination times (for data, see chapter 4.2.4.3). The width,  $W$ , of the space charge is a function of the doping concentration  $N_B$  and the applied voltage  $V$ :

$$W = \sqrt{\frac{2 \times \epsilon_s \times (V_{bi} + V)}{q \times N_B}}$$

(for a one-sided abrupt junction), where  $V_{bi}$  is the built-in voltage,  $\epsilon_s$  the dielectric constant of Si, and  $q$  the electronic charge. The capacitance of the diode, which can be speed limiting, is also a function of space charge width and applied voltage and is given by

$$C = \frac{\epsilon_s \times A}{W} \quad (1.2)$$

where  $A$  is the area of the diode. An externally applied bias will increase the space charge width (see figure 4.2b) with the result that a larger number of carriers are generated inside this zone which can be swept out very fast with high efficiency under the applied field. From equation 1.1, it is evident that the space charge width is a function of the doping concentration  $N_B$ . Diodes with a so called pin structure show a wide space charge width where  $i$  stands for intrinsic, very low doped. This zone is also sometimes nominated as  $v$  or  $p$  rather than low doped  $n$ ,  $n^-$  or  $p$ ,  $p^-$  zone indicating the very low doping.

In figure 4.6 the different behavior of low doped pin diodes and pn diodes is shown. The space charge width of the pin diode (b) with a doping level ( $n=N_B$ ) as low as  $N_B = 5 \cdot 10^{11} \text{ cm}^{-3}$  is about  $80 \mu\text{m}$  wide for a 2.5 V bias in comparison with a pn diode with a doping ( $n$ ) of  $N_B = 5 \cdot 10^{15} \text{ cm}^{-3}$  with only  $0.8 \mu\text{m}$ .

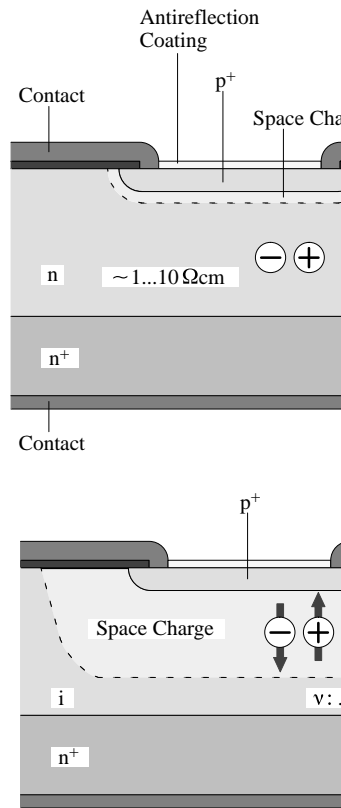


Figure 4.6. Comparison of pn diode (a) and pin diode (b)

## 4.2.2 Properties of silicon photodiodes

### 4.2.2.1 I-V Characteristics of illuminated pn junction

The I-V-characteristics of a photodiode are shown in figure 4.7. The characteristic of the non illuminated diode is identical to the

characteristic of a standard rectifier diode. The relationship between current,  $I$ , and voltage,  $V$ , is given by

$$I = I_s \times (\exp V/V_T - 1) \quad (2.1)$$

with  $V_T = kT/q$   
 $k = 1.38 \cdot 10^{-23} \text{ JK}^{-1}$ , Boltzmann constant  
 $q = 1.6 \cdot 10^{-19} \text{ As}$ , electronic charge.

$I_s$ , the dark reverse saturation current, is a material and technology dependent quantity. The value is influenced by the doping concentrations at the pn junction, by the carrier lifetime, and especially by the temperature. It shows a strongly exponential temperature dependence and doubles every  $8^\circ\text{C}$ .

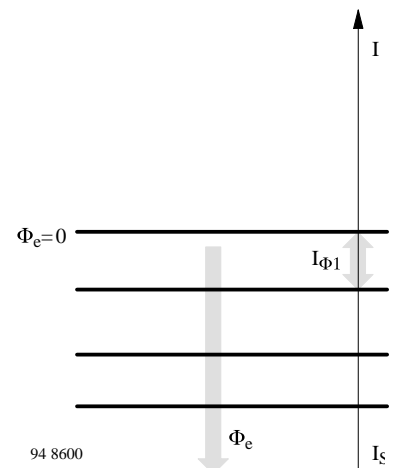


Figure 4.7a. I-V-Characteristics of an Si photodiode under illumination. Parameter: Incident radiant flux

94 8601

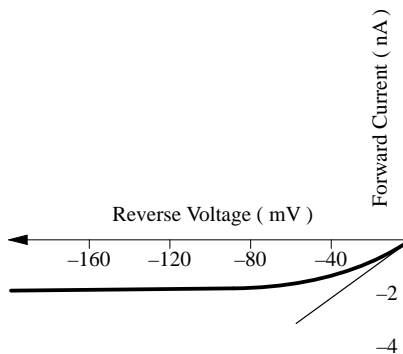


Figure 4.7b. Measured I-V-characteristics of an Si photodiode (as example S 206 P) in the vicinity of the origin

Typical dark currents of Si photodiodes are dependent on size and technology and range from less than picoamps up to tens of nanoamps at room temperature conditions. As noise generators, the dark current  $I_{r0}$  and the shunt resistance  $R_{sh}$  (defined and measured at a voltage of 10 mV forward or reverse, or peak to peak) are limiting quantities when detecting very small signals.

The photodiode exposed to optical radiation generates a photocurrent  $I_r$  exactly proportional to the incident radiant power  $\Phi_e$ . The quotient of both is the spectral responsivity  $s(\lambda)$ ,

$$s(\lambda) = I_r / \Phi_e \text{ [A/W]} \quad (2.2)$$

The characteristics of the irradiated photodiode is then given by

$$I = I_s \times (\exp V / V_T - 1) - s(\lambda) \times \Phi_e$$

and in the case  $V \approx 0$ , zero or reverse bias we find,

$$I = -I_s - s(\lambda) \times \Phi_e$$

Dependent on load resistance,  $R_L$ , and applied bias, one can distinguish different operating modes. The unbiased diode operates in the photovoltaic mode. Under short circuit conditions (load  $R_L = 0 \Omega$ ), the short circuit current,  $I_{SC}$  will flow into the load. When  $R_L$  increases to infinity the output voltage of the diode will rise to the open circuit voltage,  $V_{OC}$ , given by

$$V_{OC} = V_T \times \ln (s(\lambda) \times \Phi_e / I_s)$$

Because of this logarithmic behavior, the open circuit voltage is often used for optical lightmeters in photographic applications. The open circuit voltage shows a strong temperature dependence with a negative temperature coefficient. The reason for this is the exponential temperature coefficient of the dark reverse saturation current  $I_s$ . For precise light measurement, a temperature control of the photodiode is employed. Precise linear optical power measurements require small voltages at the load typically smaller than about 5% of the corresponding open circuit voltage. For less precise measurements, an output voltage of half the open circuit voltage can be allowed. The most important disadvantage of operating in the photovoltaic mode is the relative large response time. For faster response, it is necessary to implement an additional voltage source reverse biasing the photodiode. This mode of operation is termed the photoconductive mode. In this mode, the lowest detectable power is limited by the shot noise of the dark current,  $I_s$ , while in the photovoltaic mode, the thermal (Johnson) noise of the shunt resistance,  $R_{sh}$ , is the limiting quantity.

## 4.2.2.2 Spectral responsivity

### 4.2.2.2.1 Efficiency of Si photodiodes

The spectral responsivity,  $s_\lambda$ , is given as the number of generated charge carriers ( $\eta \cdot N$ ) per incident photons  $N$  of energy  $h \cdot \nu$  ( $\eta$  is the percent efficiency,  $h$  is Plancks constant, and  $\nu$  is the frequency of radiation). Each photon will at most generate one charge carrier. The photocurrent  $I_{re}$  then, is

$$I_{re} = \eta \times N \times q$$

$$s_\lambda = I_{re} / \Phi_e$$

$$= \eta \times N \times q / (h \times \nu \times N)$$

$$s_\lambda = \frac{\lambda(\mu m)}{1.24} \text{ [A/W]}$$

With fixed efficiency, a linear relationship between wavelength and spectral responsivity is valid.

Figure 4.4 shows that semiconductors absorb radiation similar to a cutoff filter. At wavelengths smaller than the cutoff wavelength the incident radiation is absorbed. At larger wavelengths the radiation passes through the material without interaction. The cutoff wavelength corresponds to the bandgap of the material. As long as the energy of the photon is larger than the bandgap, carriers can be generated by absorption of photons, provided that the material is thick enough to propagate photon-carrier interaction. Bearing in mind that the energy of photons decreases with increasing wavelength, it can be understood, that the curve of the spectral responsivity vs. wavelength in the ideal case (100% efficiency) will have a triangular shape (see figure 4.8). For silicon photodetectors, the cutoff wavelength is near 1100 nm.

In most applications it is not necessary to detect radiation with wavelengths larger than 1000 nm. Therefore, designers work with a typical chip thickness of 200  $\mu\text{m}$  to 300  $\mu\text{m}$ , which results in reduced sensitivity at wavelengths larger than 950  $\mu\text{m}$ . With a typical chip thickness of 250  $\mu\text{m}$ , an efficiency of about 35% at 1060 nm is achieved. At shorter wavelengths (blue-near UV, 500 nm to 300 nm) the sensitivity is limited by recombination effects near the surface of the semiconductor. The reduction in the efficiency starts near 500 nm and increases with decreasing wavelength. Standard detectors designed for visible and near IR radiation may have only poor UV/blue sensitivity and poor UV stability. Well designed sensors for wavelengths of 300 to 400 nm can operate with fairly high efficiencies. At smaller wavelengths ( $< 300$  nm) the efficiency decreases strongly.

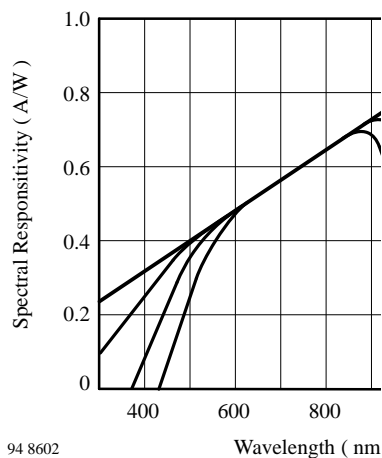


Figure 4.8. Spectral responsivity as a function of wavelength of a Si photodetector diode, ideal and typical values

#### 4.2.2.2.2 Temperature dependence of spectral responsivity

The efficiency of carrier generation by absorption and the loss of carriers by recombination are the factors which influence the spectral responsivity. The absorption coefficient increases with temperature. Radiation of long wavelength is, therefore, more efficiently absorbed inside the bulk, resulting in increasing response. For shorter wavelengths ( $< 600$  nm), reduced efficiency is observed with increasing temperature because of increased recombination rates near the surface. These effects are strongly dependent on technological parameters and therefore cannot be generalized to the behavior at longer wavelengths.

#### 4.2.2.2.3 Uniformity of spectral responsivity

Inside the technologically defined active area of photodiodes, the spectral responsivity shows a variation of the sensitivity on the order of  $< 1\%$ . Outside the defined active area, especially at the lateral edges of the chips, the local spectral response is sensitive to the applied reverse voltage. Additionally, this effect depends on the wavelength. Therefore, the relation between power (Watt) related spectral responsivity,  $s_\lambda$  (A/W), and power density (Watt/cm<sup>2</sup>) related spectral responsivity,  $s_\lambda$  [A/(W/cm<sup>2</sup>)] is not a constant. This relation is a function of wavelength and reverse bias.

#### 4.2.2.2.4 Stability of spectral responsivity

Si detectors for wavelengths between 500 nm and 800 nm appear to be stable over very long periods of time.

In the literature remarks can be found on instabilities of detectors in the blue, UV, and near IR under certain conditions. Thermal cycling has reversed the degradation effects. Surface effects and contamination are possible causes but are technologically well controlled.

#### 4.2.2.2.5 Angular dependence of responsivity

The angular response of Si photodiodes is given by the optical laws of reflection. The angular response of a detector is shown in figure 4.9.

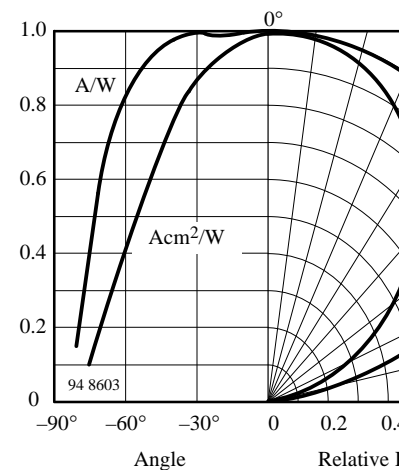


Figure 4.9. Responsivity of Si photodiodes as a function of the angle of incidence

The semiconductor surfaces are covered with quarter wavelength antireflection coatings. The encapsulation is performed with uncoated glass or sapphire windows.

The bare silicon response can be altered by optical imaging devices such as lenses. In this way nearly every arbitrary angular response can be achieved.



### 4.2.2.3 Dynamic properties of Si photodiodes

Si photodiodes are available in many different variations. The design of the diodes can be tailored for special purposes. Si photodiodes may be designed for maximum efficiency at given wavelengths, for very low leakage currents, or for high speed. The design of a photodiode is nearly always a compromise between various aspects of a specification.

Inside the absorbing material of the diode, photons can be absorbed in different regions. For example at the top of a  $p^+n^-$  Diode there is a highly doped layer of  $p^+$ -Si. Radiation of shorter wavelengths will be effectively absorbed, but for larger wavelengths only a small amount is absorbed. In the vicinity of the pn junction there is the space charge region, where most of the photons should generate carriers. An electric field accelerates the generated carrier in this part of the detector to a high drift velocity. The carriers which are not absorbed in these regions will penetrate into the field-free region, where the motion of the generated carriers fluctuates by the slow diffusion process.

The dynamic response of the detector is composed of the different processes which transport the carriers to the contacts. The dynamic response of photodiodes is influenced by three fundamental effects:

1. Drift of carriers in an electric field
2. Diffusion of carriers
3. Capacitance \* load resistance

The carrier drift in the space charge region occurs rapidly with very small time constants. Typically, the transit times in an electric field of  $0.6 \text{ V}/\mu\text{m}$  are in the order of  $16 \text{ ps}/\mu\text{m}$  and  $50 \text{ ps}/\mu\text{m}$  for electrons and holes, respectively. At the (maximum) saturation velocity, transit time is on

the order of  $10 \text{ ps}/\mu\text{m}$  for electrons in p-material. With a  $10 \mu\text{m}$  drift region, travelling times of  $100 \text{ ps}$  can be expected. The response time is a function of the distribution of the generated carriers and is, therefore, wavelength dependent.

The diffusion of carriers is a very slow process. The time constants are on the order of some  $\mu\text{s}$ . The typical pulse response of detectors is dominated by these two processes. Obviously, carriers should be absorbed in large space charge regions with high internal electrical fields. This requires material with an adequate low doping level. Furthermore, a reverse bias of rather large voltage is useful. Radiation of shorter wavelength is absorbed in smaller penetration depths. At wavelengths shorter than  $600 \text{ nm}$ , decreasing wavelength leads to an absorption in the diffused top layer. The movement of carriers in this region is also diffusion limited. Because of small carrier lifetimes, the time constants are not as large as in homogeneous substrate material. Finally, the capacitive loading of the output in combination with the load resistance limits the frequency response.

## 4.2.3 Characteristics of other silicon photodetectors

### 4.2.3.1 Avalanche photodiodes

In Avalanche photodiodes (APD) the reverse bias voltage can be increased to a value where multiplication of carriers starts by impact ionization. The amplification  $M$  can rise up to a factor of thousands, but typical working points are between  $M = 50$  and  $M = 200$ . The current gain-bandwidth product can be on the order of  $200 \text{ GHz}$ . Therefore, APDs can be used with frequencies of up to some gigahertz. A typical structure of an APD is shown in figure 4.10. The

operating reverse-bias voltage is usually between  $130$  and  $300 \text{ V}$  and must be very well controlled by a gain control circuit because of the large temperature coefficient of the multiplication factor. Sometimes, instead of a gain control, a temperature stabilization of the APD is used.

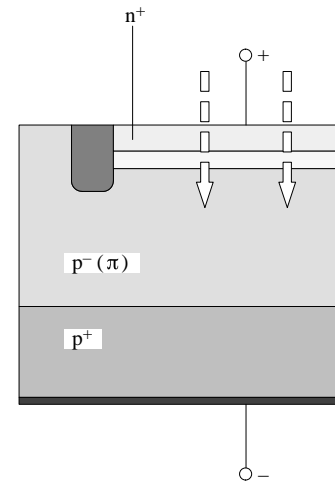


Figure 4.10. Avalanche photodiode, cross section.

### 4.2.3.2 Phototransistors

The phototransistor is equivalent to a photodiode in conjunction with a bipolar transistor amplifier (figure 4.11). Typically, current amplification,  $B$ , is between  $100$  and  $1000$  depending on the type and application. The active area of the phototransistor is usually about  $0.5 \times 0.5 \text{ mm}^2$ . Data of spectral responsivity are equivalent to those of photodiodes, but must be multiplied by the factor of the current amplification,  $B$ .

The switching times of phototransistors are dependent on the current amplification and load resistance and are between  $30 \mu\text{s}$  and  $1 \mu\text{s}$ . The resulting cutoff frequencies are a few hundred Kilohertz.

The transit times,  $t_r$  and  $t_f$ , are given by

$$t_{r,f} = \sqrt{(1/2f_t^2)^2 + b(RC_B V)^2}$$

- $f_t$ : Transit frequency
- R: Load resistance
- $C_B$ : Base-collector capacitance,
- $b = 4 \dots 5$
- V: Amplification

The most frequent application of phototransistors is found in interrupters and opto-isolators.

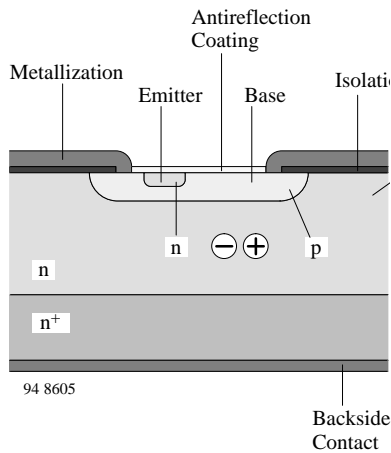


Figure 4.11. Phototransistor, cross section and equivalent circuit

## 4.2.4 Applications

Silicon photodetectors are used in manifold applications, such as sensors for radiation from the near UV over the visible to the near infrared. There are numerous applications in the measurement of light, such as dosimetry in the UV, photometry, and radiometry. A well known application is shutter control in cameras.

Another large application area for detector diodes and especially phototransistors, is that of position sensing. Examples are quadrant detectors, differential diodes, interruptors, and reflex sensors.

Other types of silicon detectors are built-in as parts of optocouplers, or optoisolators.

One of the biggest application areas, by numbers, is the remote control of TV sets and other home entertainment appliances.

Different applications require specialized detectors and also special circuits for optimized function.

### 4.2.4.1 Equivalent circuit

Photodetector diodes can be described by the electrical equivalent circuit shown in figure 4.12.

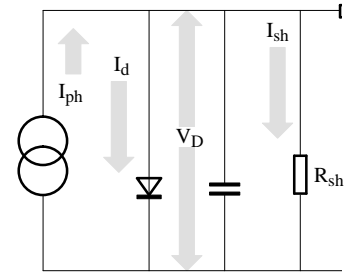


Figure 4.12

$$I_O = I_{ph} - I_D - I_{sh}$$

$$I_O = I_{ph} - I_s \left( \exp \frac{qV_D}{kT} - 1 \right) - I_{sh}$$

$$V_{OC} = V_T \times \ln \left( \frac{s(\lambda) \times \phi_e - I_{sh}}{I_s} + 1 \right)$$

As described in chapter 4.2, the incident radiation generates a photocurrent loaded by a diode characteristic and the load resistor,  $R_L$ . The other parts of the equivalent circuit (the parallel capacitance,  $C$ , combined from junction,  $C_j$ , and stray capacitances, the serial resistance,  $R_S$ , and the shunt resistance,  $R_{sh}$ , representing an additional leakage) can be neglected in most of the standard applications, and are not expressed in equations 2.3 and 2.4.

However, at the limits of the field of application, high frequencies or extreme irradiation levels, these parts must be regarded as limiting elements.

### 4.2.4.2 Searching for the right detector diode type

The photodiode BPW 20 R is a pn diode based on rather highly doped n-silicon, while the S 153 P is a pin diode based on very lightly doped n-silicon. Both diodes have the same active area and the spectral response, as a function of the wavelength, is very similar. The difference arises in the junction capacitance and shunt resistance, both of which can influence the performance in the application.

# TEMIC

TELEFUNKEN Semiconductors

---

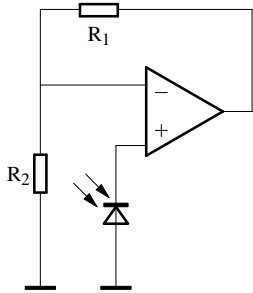
Detecting very small signals is the domain of the pn diodes with their very small dark currents and dark/shunt resistances. With a specialized detector technology, these

parameters are very well controlled on all TEMIC photodetectors.

The very small leakage currents of pn

diodes are offset by higher capacitances and smaller bandwidths in comparison to pin diodes.

Often, especially in light meters, photodiodes are operated in the photovoltaic mode, as depicted in the circuit of figure 4.13, where a strong logarithmic dependence of the open circuit voltage on the input signal is used.



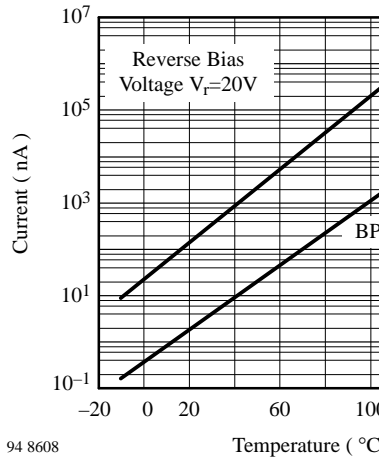
$$V_O \approx V_{OC} \times [1 + R_1/R_2]$$

$$V_{OC} = V_T \times \ln (s(\lambda) \times \phi_e / I_s + I_{sh})$$

Figure 4.13. Photodiode in the photovoltaic mode operating with a voltage amplifier

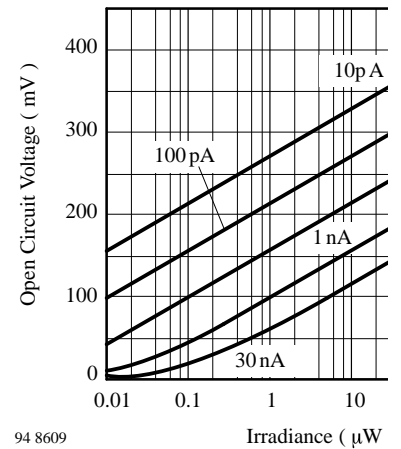
It should be noted that the extremely high shunt/dark resistance (more than 15 GΩ) combined with a high-impedance operational amplifier input and a junction capacitance of about 1 nF can result in slow switching off time constants of some seconds. Some instruments, therefore, have a reset button for shortening the diode before starting a measurement. The photovoltaic mode of operation for precise measurements should be limited to the range of low ambient temperatures or a temperature control

of the diode (e.g., using a Peltier cooler) should be implied. At elevated temperatures, the dark current is increased (see figure 4.14) leading to a non-logarithmic and temperature dependent output characteristic (see figure 4.15). The curves shown in figure 4.14 represent the typical behavior of these diodes. The guaranteed leakage (dark reverse current) is specified with  $I_{r0} = 30 \text{ nA}$  for the standard types. This value is far from that typically measured. Tighter customer specifications are available on request. The curves of figure 4.15 show the open circuit voltage as a function of the irradiance with the dark reverse current,  $I_s$ , as parameter (in a first approximation increasing  $I_s$  and  $I_{sh}$  have the same effect). The parameter covers the possible spread of dark current. In combination with figure 4.14 one can project the extreme dependence of the open circuit voltage at high temperatures.



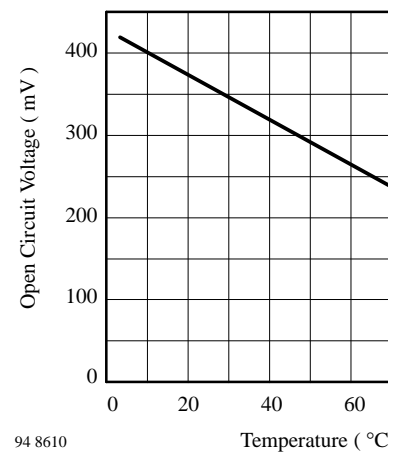
94 8608

Figure 4.14. Dark reverse current vs. temperature



94 8609

Figure 4.15. Open circuit voltage vs. irradiance, parameter: dark reverse current, BPW 20 R



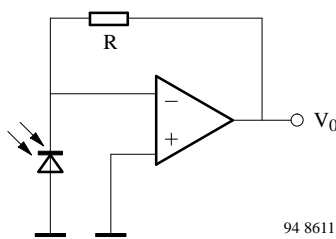
94 8610

Figure 4.16. Open circuit voltage vs. temperature, BPW46

### 4.2.4.3 Operating modes and circuits

The advantages and disadvantages of operating a photodiode in the open circuit mode have been discussed.

For operation in the short circuit (see figure 4.17) or photoconductive (see figure 4.18) mode, current-to-voltage converters are typically used. In comparison with the photovoltaic mode, the temperature dependence of the output signal is much lower. Generally, it can be stated that the temperature coefficient of the light reverse current is positive for irradiation with wavelengths  $> 900$  nm, growing with increasing wavelength. For wavelengths  $< 600$  nm, a negative temperature coefficient is found, likewise with increasing absolute value to shorter wavelengths. Between these wavelength boundaries the output is nearly independent of temperature. Using this mode of operation, reverse biased or unbiased (short circuit conditions), the output voltage,  $V_o$ , will be directly proportional to the incident radiation,  $\phi_e$  (see the equation in figure 4.17a).



$$V_o = -R \times \Phi_e \times s(\lambda)$$

$$V_o = -I_{sc} \times R$$

Figure 4.17a. Transimpedance amplifier, current to voltage converter, short circuit mode

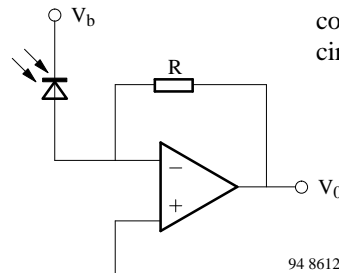


Figure 4.17b. Transimpedance amplifier, current to voltage converter, reverse biased photodiode

The circuit in figure 4.17a minimizes the effect of the reverse dark current while the circuit in figure 4.17b improves the speed of the detector diode due to a wider space charge region with decreased junction capacitance and field increased velocity of the charge carrier transport.

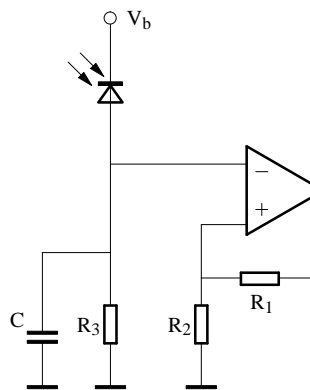
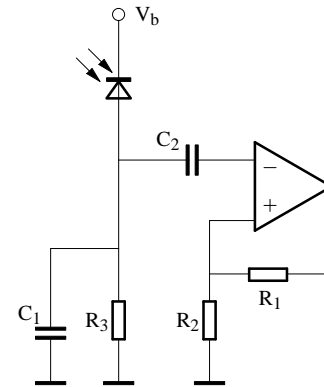


Figure 4.18. RC-loaded photodiode with voltage amplifier

Figure 4.18 shows photocurrent flowing into an RC load, where C represents the junction and stray capacitance while  $R_3$  can be a real or complex load, such as a resonant circuit for the operating frequency.



$$V_o \approx \phi_e \times s(\lambda) \times R_3 \times [1$$

Figure 4.19. AC-coupled amplifier circuit

The circuit in figure 4.19 is equivalent to figure 4.18 with a change to AC coupling. In this case, the influence of the background illumination can be separated from a modulated signal. The relation between input signal (irradiation,  $\phi_e$ ) and output voltage is given by the equation in figure 4.19.

### 4.2.4.4 Frequency response

The limitations of the switching times in pn diodes is determined by the carrier lifetime. Due to the absorption properties of silicon, especially in pn diodes, most of the incident radiation at longer wavelengths is absorbed outside the space charge region. Therefore, a strong wavelength dependence of the switching times can be observed (figure 4.20).

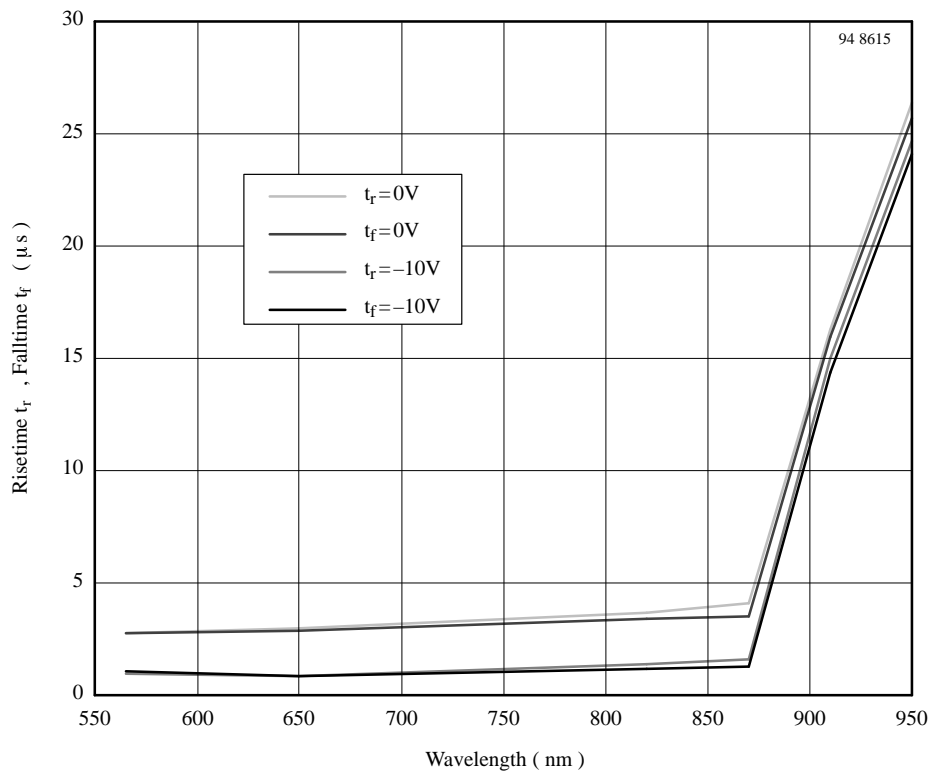


Figure 4.20. Switching times vs. wavelength for photodiode BPW 20 R

A drastic increase in rise and fall times is observed at wavelengths  $> 850$  nm. The differences between unbiased and biased operation result from the widening of the space charge region. However, for the pin diodes (BPW 34 / S 153 P family) similar results with shifted time scales are found. This behavior, in this case in the frequency domain, is presented in figure 4.21 for a wavelength of 820 nm and figure 4.22. for 950 nm.

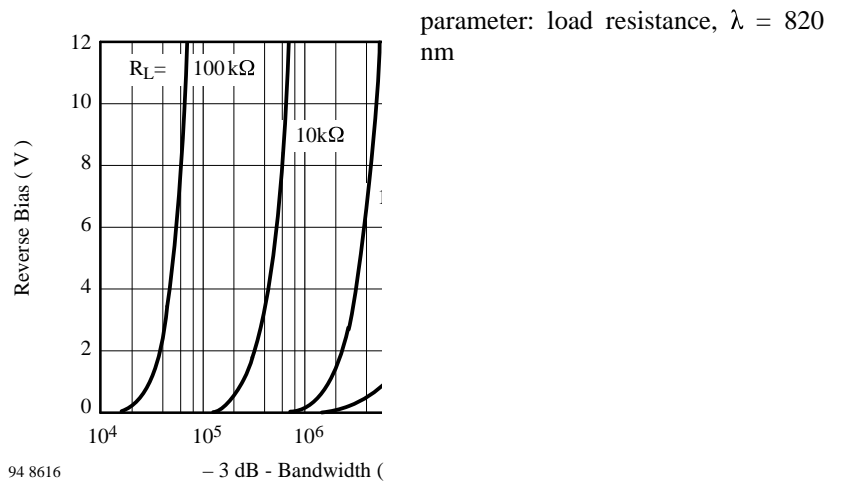


Figure 4.21. BPW 41-family, bandwidth vs. reverse bias voltage,

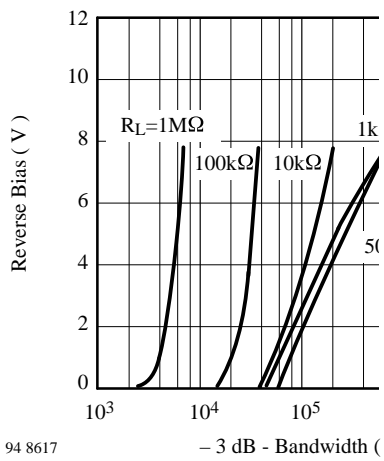


Figure 4.22. BPW 41-family, bandwidth vs. reverse bias voltage, parameter: load resistance,  $\lambda = 950$  nm

Below about 870 nm only a small wavelength dependence can be recognized while a steep change of cut-off frequency takes place from 870 nm to 950 nm (different time scales in figure 4.21 and figure 4.22!).

Additionally, the influence of the load resistances and the reverse bias voltages can be taken from these diagrams.

For cutoff frequencies greater 10–20 MHz, depending on the supply voltage available for biasing the detector diode, pin diodes are also used. However, for this frequency range, and especially when operating with low bias voltages, thin epitaxially grown intrinsic (i) layers are incorporated in the pin diodes. As a result, these diodes (e.g., TEMICs BPW 97) can operate with low bias voltages (3 to 4 V) with cutoff frequencies of 300 MHz at a wavelength of 790 nm. With application specific optimized

designs, we are able to supply pin diodes with cutoff frequencies up to 1 GHz at only a 3 V bias voltage with only an insignificant loss of responsivity.

For operating these fast diodes in combination with current voltage converters, transimpedance amplifiers, signal regenerators and LED drivers are available from TEMIC (Transimpedance amplifier: U 6791, regenerator: U 6792, and LED driver: U 6795).

The main applications for these photodiodes are found in optical local area networks operating in the first optical window at wavelengths of 770 nm to 880 nm.

#### 4.2.4.5 Which type for which application?

In table 4.2 selected diode types are assigned to different applications. For more precise selection according to chip sizes and packages refer to the tables on the introductory pages of this data book.

Table 4.2 Diode reference table

Detector application	pin diode	pn diode	epi-pin diode
Photometry, Lightmeter		BPW 21 R	
Radiometry	S 153 P, BPW 34, ...	BPW 20 R	
Light barriers	BPW 24		
Remote control Low speed data transmission < 10 MHz, clear package	BPW 34, BPW 46, BPV 10		
IR filter for $\lambda > 900$ nm included	BPV 20 F–BPV 23 F, BPW 41 N, S 186 P, BPV 10 F, S 288 P, TFM-Series (with integrated amplifier and demodulator)		
IR filter for $\lambda > 820$ nm included	BPV 23 NF, BPW 82, BPW 83		
Fiber optical receiver	frequencies < 20 MHz BPW 88, BPW 24		high frequencies BPW 97, BPW 98
Densitometry	BPW 34, BPV 10, BPW 43	BPW 20 R, BPW 21 R	
Quadrant detector		S 239 P	

## 4.2.5 Phototransistors

### 4.2.5.1 Circuits

Typically a phototransistor is operated in a circuit as shown in figure 4.23. The resistor  $R_B$  can be omitted in most applications. In some phototransistors the base is not connected.  $R_B$  can be used to suppress background radiation by setting a

threshold level (see equation 5.1 and 5.2)

$$V_O = V_S - B \times \phi_e \times s(\lambda) \times R_L$$

$$V_O \approx V_S - (B \times \phi_e \times s(\lambda) - 0.6/R$$

For the dependence of the rise and fall times on the load resistance and collector-base capacitance refer to chapter 4.2.3.2.

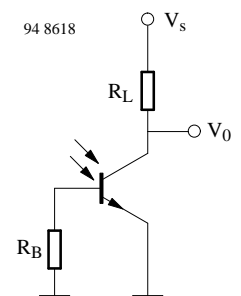


Figure 4.23. Phototransistor with load resistor and optional base resistor.



## 5. Measurement techniques

### 5.1 Introduction

The characteristics of optoelectronics devices given in the data sheets are verified either by 100% production tests followed by statistic evaluation or by sample tests on typical specimens. These tests can be divided into the following categories:

- a) Dark measurements
- b) Light measurements
- c) Measurements of switching characteristics, cut-off frequency and capacitance
- d) Angular distribution measurements
- e) Spectral distribution measurements
- f) Thermal measurements.

The dark and light measurements are 100% measurements. All other values are typical. The basic circuits used for these measurements are shown in the following sections. The circuits may be modified slightly to cater for special measurement requirements.

Most of the test circuits may be simplified by use of a Source Measure Unit (SMU), which allows either to source voltage and measure current or to source current and measure voltage.

### 5.2 Dark and light measurements

#### 5.2.1 Emitter devices

##### 5.2.1.1 IR diodes (GaAs)

The forward voltage,  $V_F$  is measured either on a curve tracer or statically using the circuit shown in figure 5.1. A specified forward current (from a constant current source) is passed

through the device and the voltage developed across it is measured on a high-impedance voltmeter.

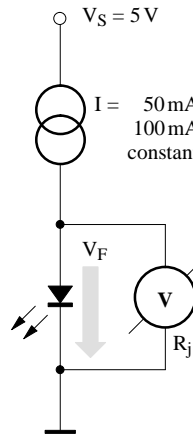


Figure 5.1

To measure the reverse voltage,  $V_R$ , a  $10 \mu\text{A}$  or  $100 \mu\text{A}$  reverse current from a constant current source is impressed through the diode (figure 5.2) and the voltage developed across it is measured on a voltmeter of high input impedance ( $\geq 10\text{M}\Omega$ ).

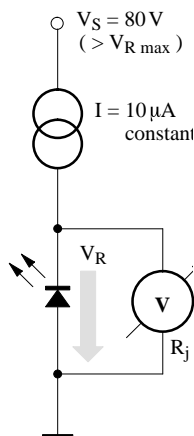


Figure 5.2

For most devices,  $V_R$  is specified at  $10 \mu\text{A}$  reverse current. In this case either

a high impedance voltmeter has to be used, or the current consumption of the DVM has to be calculated and added to the specified current. A second measurement step will then give correct readings.

In the case of GaAs IR diodes, it is usual to measure the total radiant output power,  $\Phi_e$ . This is done with a calibrated large-area photovoltaic cell fitted in a conical reflector with a bore which accepts the test item – see figure 5.3. An alternate test set uses a silicon photodiode attached to an integrating sphere. A constant dc or pulsating forward current of specified magnitude is passed through the IR diode. The advantage of pulse current measurements at room temperature ( $25^\circ\text{C}$ ) is that the results can be reproduced exactly. If, for reasons of measurement economy, only dc measurements (figure 5.4) are to be made, then the energizing time should be kept short (below 1 s) and of uniform duration, to minimize any fall-off in light output due to internal heating.

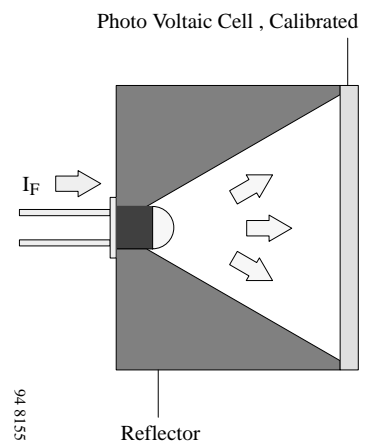


Figure 5.3

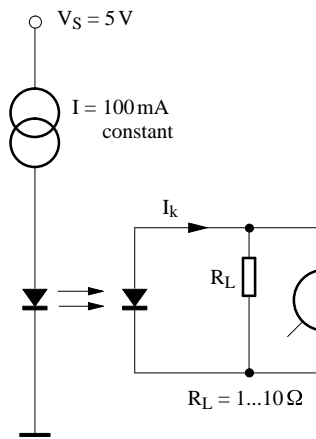


Figure 5.4

To ensure that the relationship between irradiance and photocurrent is linear, the photodiode should operate near short-circuit configuration. This can be achieved by using a low resistance load ( $\leq 10 \Omega$ ) of such a value that the voltage dropped across it is very much lower than the open circuit voltage produced under identical illumination conditions ( $R_{meas} \ll R_i$ ). The voltage across the load should be measured with a sensitive DVM.

Knowledge of the radiant intensity,  $I_e$ , produced by an IR emitter enables customers to assess the range of IR light barriers. The measurement procedure for this is more or less the same as that used for measuring the radiant power. The only difference is that in this case the photodiode is used without a reflector and is mounted at a specified distance from, and on the

optical axis of, the IR diode (figure 5.5) so that only radiant power of a narrow axial beam is considered. The radiant power within a solid angle of  $\Omega = 0.01$  steradian (sr) is measured at a distance of 100 mm. The radiant intensity is then obtained by using this measured value for calculating the radiant intensity for a solid angle of  $\Omega = 1$  sr.

### 5.2.1.2 Light emitting diodes

For forward and reverse voltage measurements ( $V_F$  and  $V_R$  respectively) refer to section 5.2.1.1, IR diodes.

The luminous intensity,  $I_v$  of a light emitting diode can be calculated by multiplying the radiant intensity,  $I_e$ , (figure 5.5) by the absolute eye sensitivity,  $K_m \times V(\lambda)$  (DIN 5031). This assumes, however, that the wavelength of the radiation emitted by the test item is known exactly. In production measurements, a calibrated silicon photovoltaic cell is used in conjunction with a special color filter (e.g., Schott BG 38) which simulates the red-slope of the eye sensitivity curve. BPW 20 R is used as a photovoltaic cell because the short circuit output current characteristic of this cell is strictly linear even when the irradiation is very low. This is because the radiant output power of LEDs is low in comparison with that of IR diodes, and the color filter has an attenuating effect causing the cell to produce, at the most, only a few

nanoamperes. The cell must operate into an operational amplifier with a high-impedance FET input stage (figure 5.6). Alternately a high sensitive electrometer may be used.

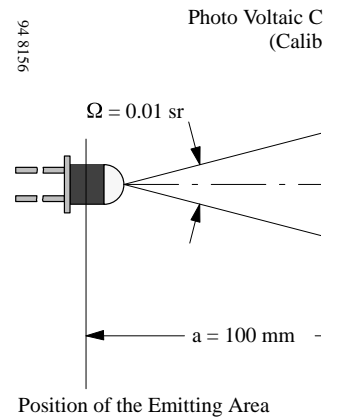


Figure 5.5

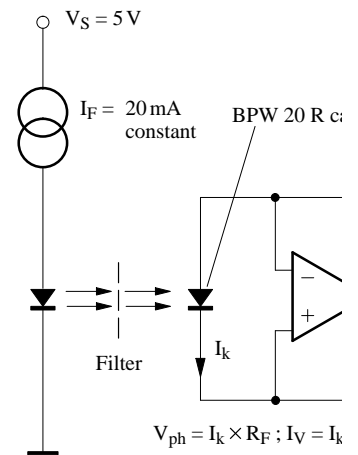


Figure 5.6

## 5.2.2 Detector devices

### 5.2.2.1 Photovoltaic cells, photodiodes

#### a) Dark measurements

The reverse voltage characteristic,  $V_R$ , is measured either on a curve tracer or statically using the circuit shown in figure 5.7. A high-impedance voltmeter, which draws only an insignificant fraction of the device's reverse current, must be used.

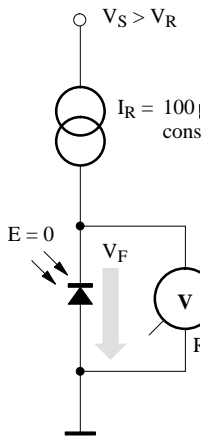


Figure 5.7

Dark reverse current measurements,  $I_{R0}$ , must be carried out in complete darkness – the reverse currents of silicon photodiodes are of the order of nanoamperes only, and an illumination of a few lux is quite sufficient to falsify the test result. If a highly sensitive DVM is to be used, then a current sampling resistor of such a value that the voltage dropped across it is small in comparison with the supply voltage must be connected in series with the test item (figure 5.8). Under these conditions any reverse voltage variations of the test samples can be ignored. Shunt resistance (dark resistance) is determined by applying

of very small voltage to the photodiode and then measuring the dark current. In case of 10 mV or less, forward and reverse polarity will result in similar readings.

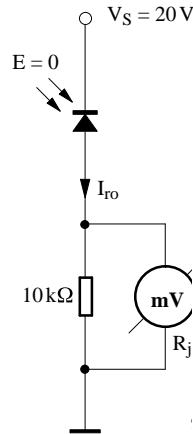


Figure 5.8

#### b) Light measurements

The same circuit used in the dark measurement can be used to carry out light reverse current,  $I_{Ra}$ , measurements on photodiodes. The only difference is that the diode is now irradiated and a current sampling resistor of lower value must be used (figure 5.9), because of the higher currents involved.

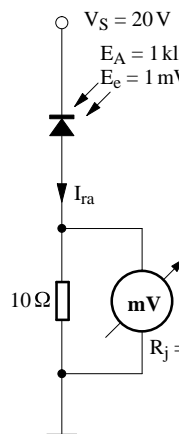
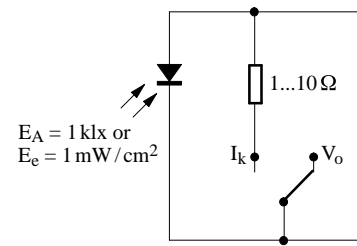


Figure 5.9

The open circuit voltage,  $V_0$ , and short circuit current,  $I_k$ , of photovoltaic cells and photodiodes are measured by means of the test circuit shown in figure 5.10. The value of the load resistor used for the  $I_k$  measurement should be chosen so that the voltage dropped across it is low in comparison with the open circuit voltage produced under conditions of identical irradiation.



94 8212

Figure 5.10

The light source used for light measurements is a calibrated incandescent tungsten lamp with no filters. The filament current is adjusted for a color temperature of 2856 K (standard illuminant A to DIN 5033 sheet 7), and the specified illumination,  $E_v$ , (usually 100 or 1000 lux) is produced by adjusting the distance,  $a$ , between the lamp and the detector on an optical bench.  $E_v$  can be measured on a  $V(\lambda)$ -corrected lux meter, or, if the luminous intensity,  $I_v$ , of the lamp is known,  $E_v$  can be calculated using the formula:  $E_v = I_v/a^2$ .

It should be noted that this inverse square law is only strictly accurate for point light sources, that is for sources where the dimensions of the source (the filament) are small ( $\leq 10\%$ ) in comparison with the distance between source and detector.

Since lux is a measure for visible light only, near infrared radiation (800 to 1100 nanometers) where silicon detectors have their peak sensitivity, is not taken into account. Unfortunately, near infrared emission of filament lamps of different construction varies widely. As a result, light current measurements done with different lamps (but the same lux and color temperature calibration) may give readings that differ up to 20%.

The simplest way to overcome this problem is to calibrate (measure the light current) some items of a photodetector type with a standard lamp (OSRAM WI41G) and then take these devices for adjustment of the lamp used for field measurements.

An IR diode is used as a radiation source (instead of the tungsten incandescent lamp), to measure detector devices being used mainly in IR transmission systems together with IR emitters (e.g. IR remote control, IR headphone). Operation is possible both with dc or pulsed current.

The adjustment of irradiance,  $E_e$ , is similar to the above mentioned adjustment of illuminance,  $E_v$ . To achieve a high stability similar to the

filament lamps, consideration should be given to the following two points:

- The IR emitter should be connected to a good heat sink to provide sufficient temperature stability.
- dc or pulse current levels as well as pulse duration have great influence on the self heating of IR diodes and should be chosen carefully.
- The radiant intensity,  $I_e$ , of the device is permanently controlled by a calibrated detector.

### 5.2.2.2 Phototransistors, photodarlington transistors

The collector emitter voltage,  $V_{CE0}$ , is measured either on a transistor curve tracer or statically using the circuit shown in figure 5.11. Normal bench illumination does not change the measuring result.

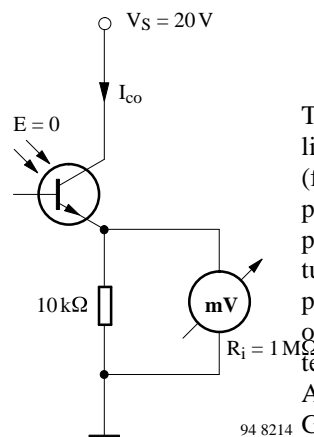


Figure 5.11

In contrast, however, the collector dark current,  $I_{CE0}$  or  $I_{C0}$ , must be

measured in complete darkness (figure 5.12). Even ordinary daylight illumination of the wire feed-through glass seals would falsify the measurement result.

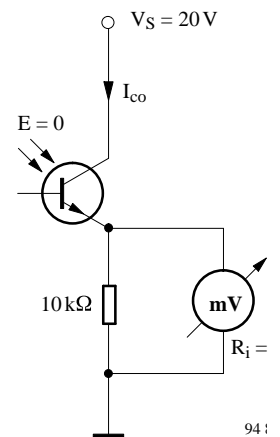


Figure 5.12

The same circuit is used for collector light current,  $I_{ca}$ , measurements (figure 5.13), the device being positioned so that its optical axis points towards an incandescent tungsten lamp with no filters, producing a standard-A illuminance of 100 or 1000 lx with a color temperature of  $T_f = 2856$  K. Alternately an IR irradiance by a GaAs diode is used (refer to the photovoltaic cells and photodiodes section). Note that a lower value sampling resistor is used, in keeping with the higher current involved.

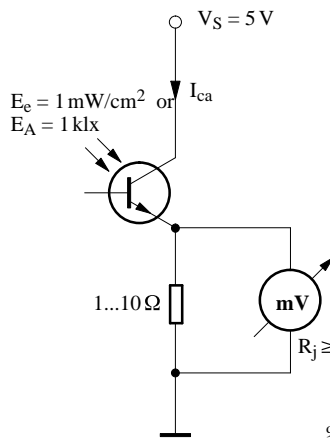


Figure 5.13

To measure the collector emitter saturation voltage,  $V_{CEsat}$ , the device is illuminated and a constant collector current passed through it. The magnitude of this current is adjusted so that it is less than the minimum light current,  $I_{ca\ min}$ , for the same illuminance (figure 5.14). The saturation voltage of the phototransistor or Darlington stage (approximately 100 mV or 600 mV, respectively) is then measured on a high impedance voltmeter.

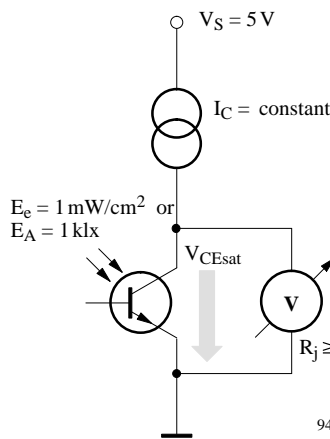


Figure 5.14

## 5.2.3 Coupling devices

### a) Dark measurements

**Emitters:** For forward and reverse voltage measurements refer to section 5.2.1.1., IR diodes.

**Detectors:** For  $V_{CEO}$  and  $I_{co}$  measurements refer to section 5.2.2.2., phototransistors.

### b) Light measurements

To measure the collector current,  $I_C$  (figure 5.15), a specified forward current,  $I_F$ , is impressed with the IR emitter. Voltage difference is then measured across a low emitter resistance. In the case of collector emitter saturation voltage,  $V_{CEsat}$  (figure 5.16), forward current,  $I_F$ , in the IR diode, and a low collector current,  $I_C$ , in the phototransistor, are impressed.  $V_{CEsat}$  is then measured (across collector and emitter terminals) as shown in the diagram.

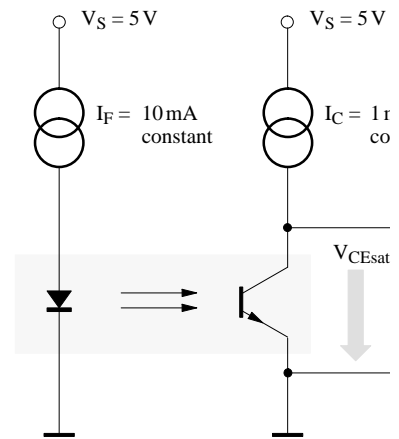


Figure 5.16

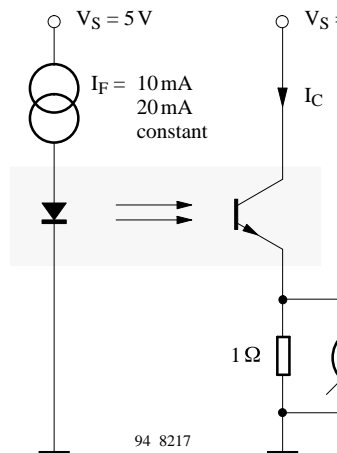


Figure 5.15

## 5.3 Switching characteristics

### 5.3.1 Definition

Every electronic device introduces a certain delay between input and output signals as well as a certain amount of amplitude distortion. The simplified circuit shown in figure 5.17 shows how the input and output signals of opto electronic devices can be displayed on a dual trace oscilloscope.

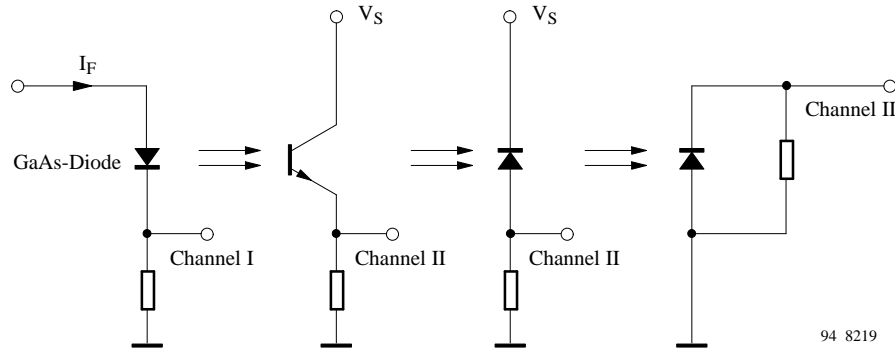


Figure 5.17

The switching characteristics can be determined by comparing the timing of the output current waveform with that of the input current waveform (figure 5.18).

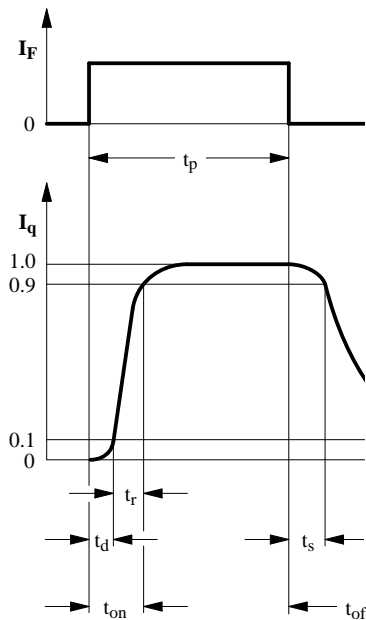


Figure 5.18

These time parameters also include the delay that exists in a luminescence diode between the forward current ( $I_F$ ) and the radiant power ( $\Phi_e$ ).

### 5.3.2 Notes concerning the test set-up

The circuits used for testing light emitting, light sensitive and optically coupled isolator devices are basically the same (figure 5.17), the only difference being the way in which the test item is connected in the circuit.

It is assumed that the rise and fall times associated with the signal source (pulse generator) and the dual trace oscilloscope are insignificant, and that the switching characteristics of any light sensitive device used in the set-up are considerably shorter than those of the test item. The switching characteristics of light and IR emitters, for example ( $t_r \approx 10$  to  $1000$  ns) are measured with the aid of a pin photodiode as a detector ( $t_r \approx 1$  ns).

Photo and darlington transistors and photo and solar cells ( $t_r \approx 0.5$  to  $50 \mu s$ ) are, as a rule, measured by use of fast IR diodes ( $t_r < 30$  ns) as emitters.

GaAsP red light emitting diodes are used as light sources only for devices which cannot be measured with IR diodes because of their spectral sensitivity (e.g. BPW 21 R). This is

because these diodes emit only 1/10 of the radiant power of IR diodes and consequently generate only very low signal levels.

### 5.3.3 Switching characteristic improvements

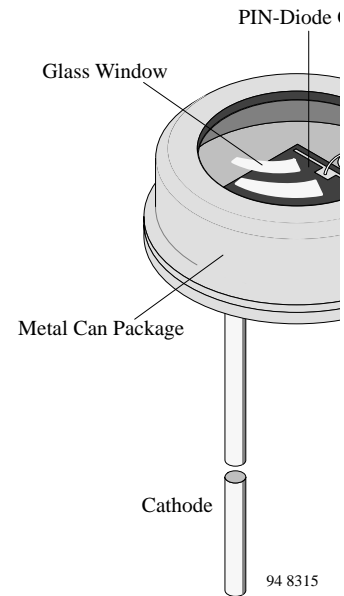
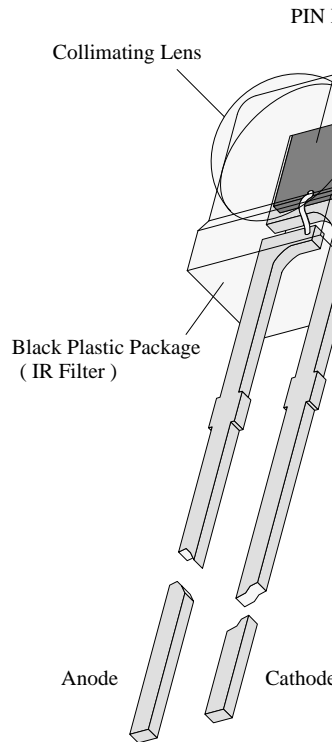
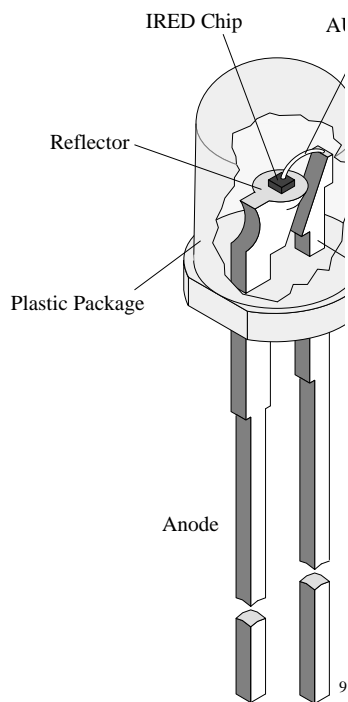
#### on phototransistors and darlington phototransistors

As in any ordinary transistor, switching times are reduced if the drive signal level, and hence the collector current, is increased. Another time reduction (especially in fall time  $t_f$ ) can be achieved by use of a suitable base resistor, assuming there is an external base connection, although this can only be done at the expense of sensitivity.

## 6. Component construction

Infrared components are available in plastic or metal packages. Plastic devices, where the chip is mounted and bonded on a lead frame, have their main advantage in lower cost and enhanced output power or sensitivity.

Devices in hermetically sealed packages have better performance in optical and mechanical tolerances and an extended operating temperature range.



## 7. Tape and reel standards

TEMIC TELEFUNKEN microelectronic offers T-1 (3 mm) and T-1<sup>3/4</sup> (5 mm) IR emitters and detectors packaged on tape. The following specification is based on IEC publication 286, taking into account the industrial requirements for automatic insertion.

Absolute maximum ratings, mechanical dimensions, optical and electrical characteristics for taped devices are identical to the basic catalog types and can be found in the specifications for untaped devices.

Note that the lead wires of taped components may be shorted or bent in accordance with the IEC standard.

### 7.1. Packing

The tapes of components are available on reels or in fan-fold boxes. Each reel and each box is marked with labels which contain the following information:

- Tfk
- Type
- Group
- Tape code (see figure 7.1.)
- Production code
- Quantity

### Code for taped IREDS

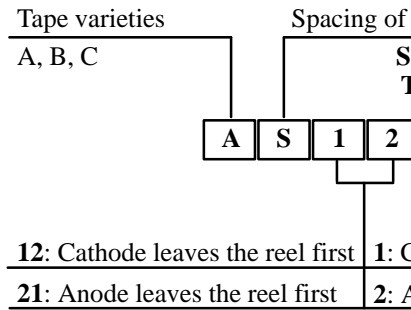


Figure 7.1 Taping code

### 7.1.1 Number of components

Quantity per reel:	3
mm IRED: 2000 pcs	5
mm IRED: 1000 pcs	3
Quantity per fan-fold box:	5
mm IRED: 2000 pcs	
mm IRED: 1000 pcs	

This results in the increments for the ordering quantities:

- 3 mm: Increments of 2000 pcs
- 5 mm: Increments of 1000 pcs

### 7.1.2. Missing components

Up to 3 consecutive components may be missing if the gap is followed by at least 3 components. A maximum of 5% of the components per reel quantity may be missing. At least 5 empty positions are present at the start and the end of the tape for tape insertion.

Z: only for fan-fold packing.  
**Tensile strength** of the tape:  $\geq 15$  N  
**Pulling force** in the plane of the tape, at right angles to the reel:  $\geq 5$  N

Note:

Shipment in fan-fold packages are standard for radial taped devices. Shipments in reel packing are only possible, if the customer guarantees the removal of empty reels. We cannot accept the return of reels according to a German wrapping decree.

### 7.2 Order designation

The type designation of the device is extended by the code shown above.

**Example:** TSIP 5200 AS12 (reel packing) or TSIP 5200 AS12Z (fan-fold packing) BPW 85 AS12 (reel packing)



**7.2.1 Tape dimensions for  $\varnothing$  3 mm standard packages**  
**available package variations: 1 2, 1 2Z, 2 1**

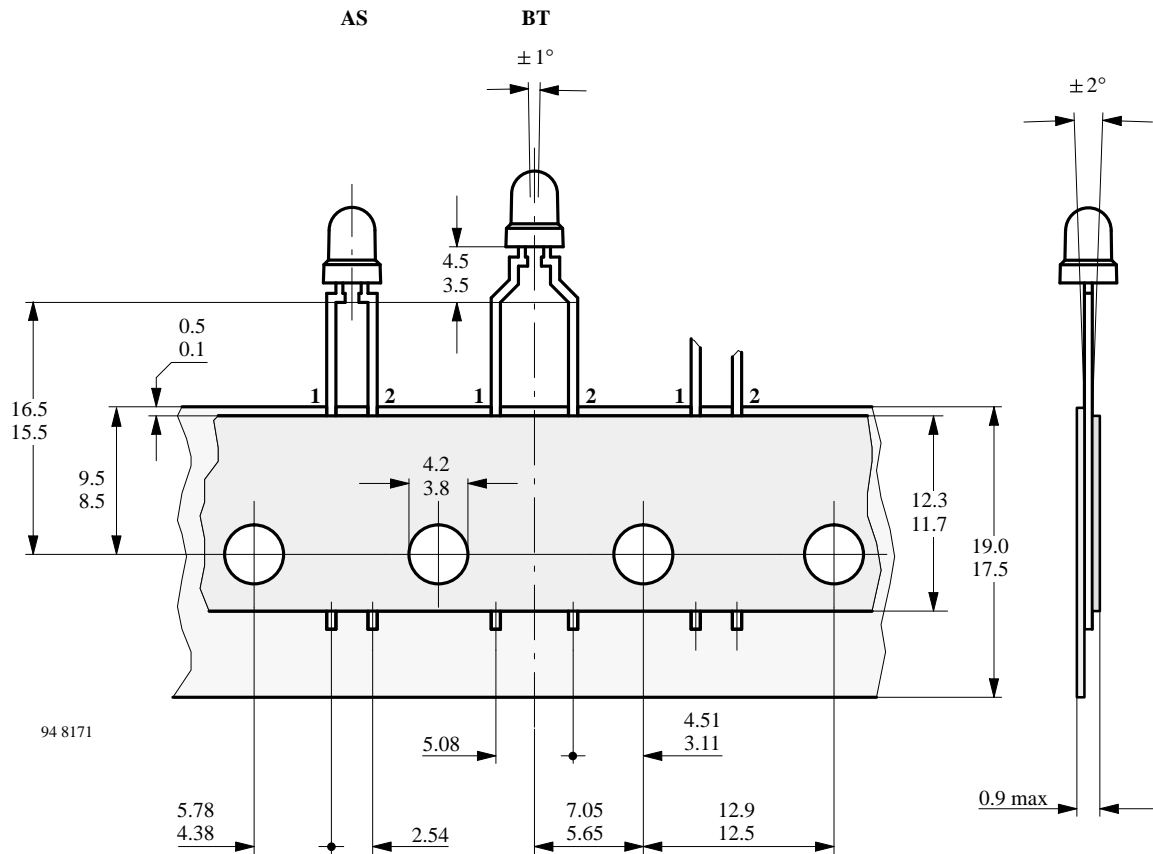


Figure 7.2 Tape dimensions  $\varnothing$  3mm devices

## 7.2.2 Tape dimensions for $\varnothing 5$ mm standard packages

available package variations: 1 2, 1 2Z, 2 1

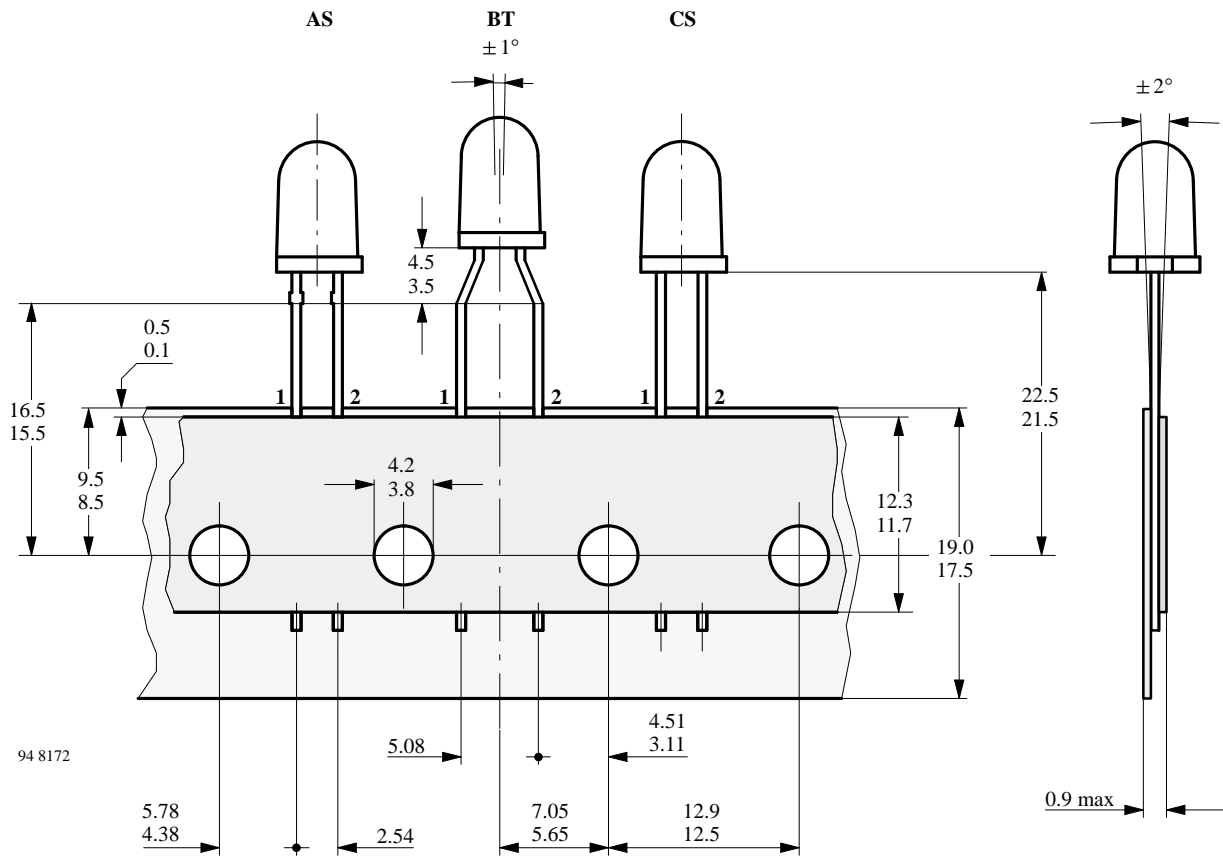
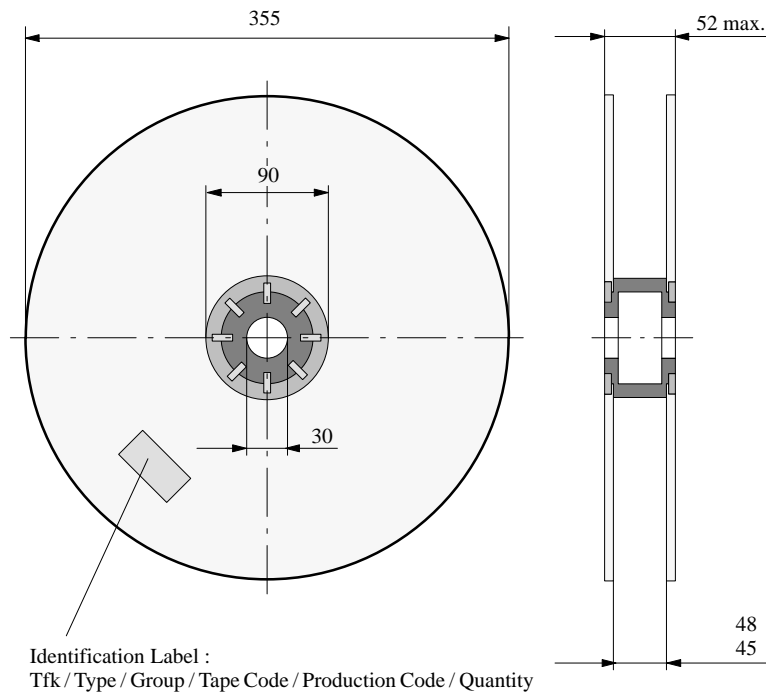


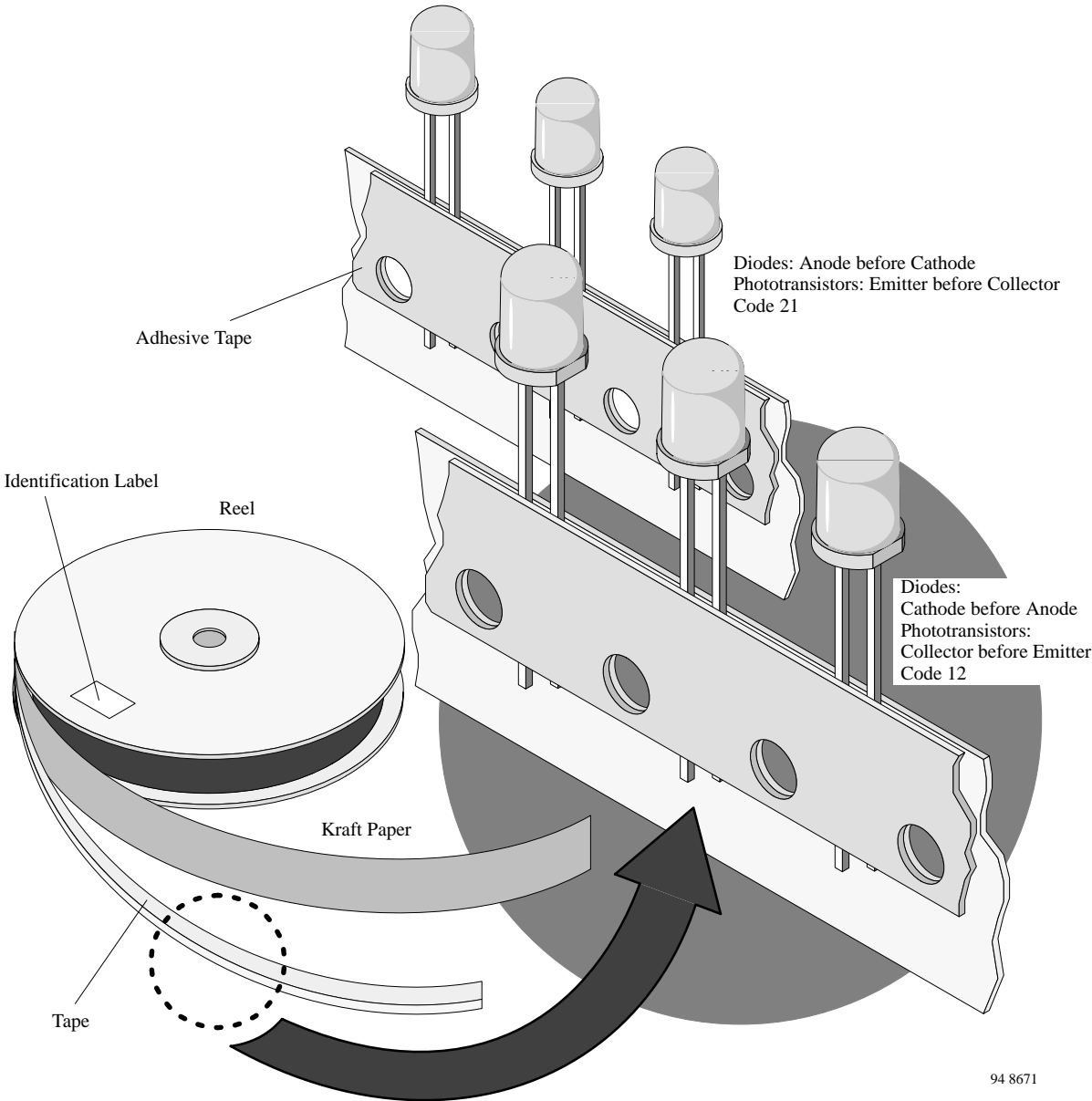
Figure 7.3 Tape dimensions  $\varnothing 5$  mm devices

## 7.2.3 Reel package, dimensions in mm



94 8641

Figure 7.4 Dimensions of the reel



94 8671

Figure 7.5 Winded devices

## 7.2.4 Fan-fold packing

The tape is folded in a concertina arrangement and it is laid in the cardboard box.

If the components are required with

the cathode before the anode (figure 7.6), the start of the tape should be taken from the side of the box marked “-”;

anode before cathode (figure 7.7), it should be taken from the side of the box marked “+”.

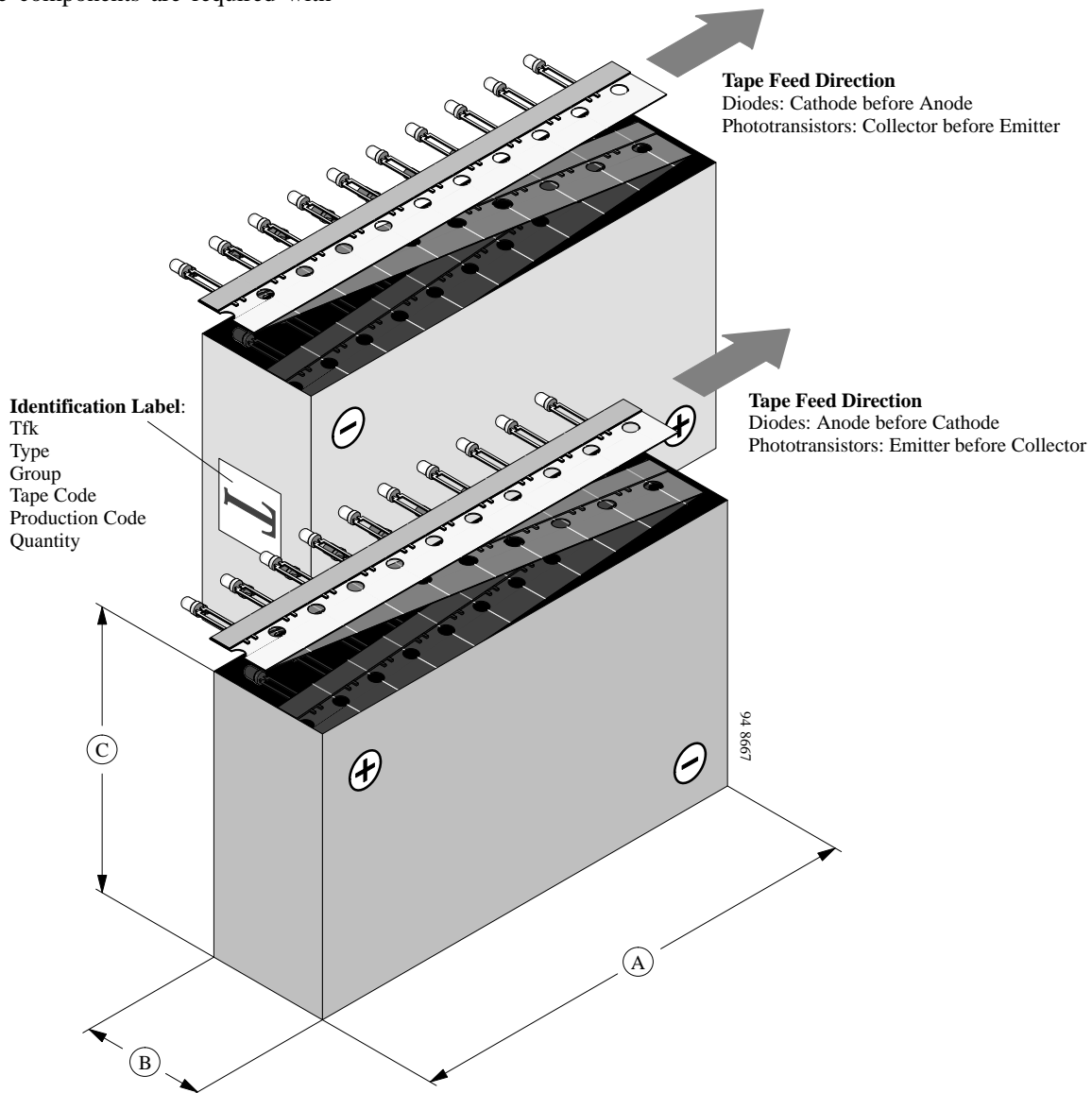


Figure 7.6 Tape direction

Table 7.1 Inner dimensions

A	B	C	Packages
34 0	46	12 5	Ø5 mm
34 0	34	16 0	Ø3 mm AS-Taping
34 0	41	16 0	Ø3 mm other than AS-Taping

## 7.3 Taping of SMT-devices

TEMIC TELEFUNKEN microelectronic IREDS and detectors in SMD packages are available in an antistatic 8 mm blister tape (in

accordance with DIN IEC 40 (CO) 564) for automatic component insertion. The blister tape

is a plastic strip with impressed component cavities, covered by a top tape.

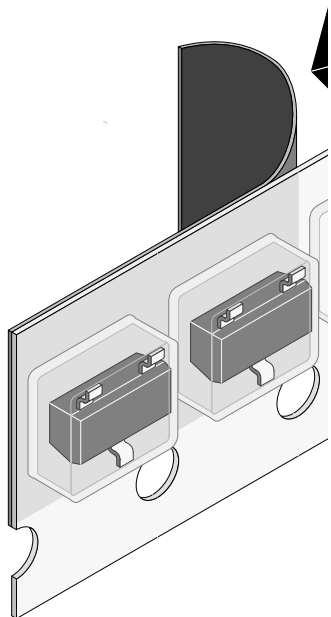
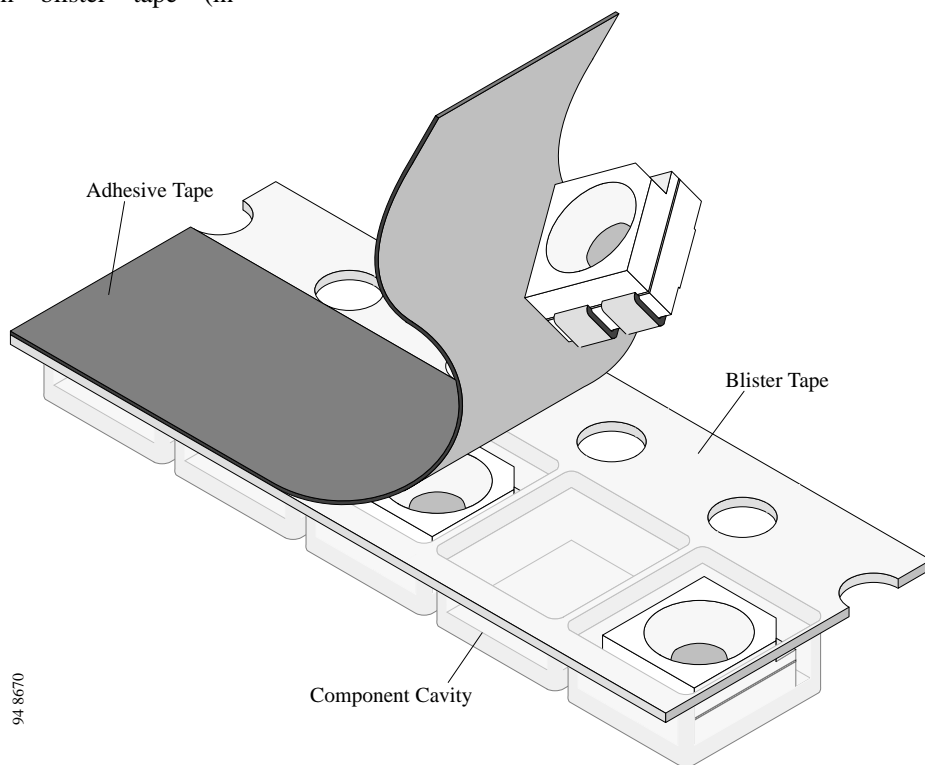


Figure 7.7 Blister tape

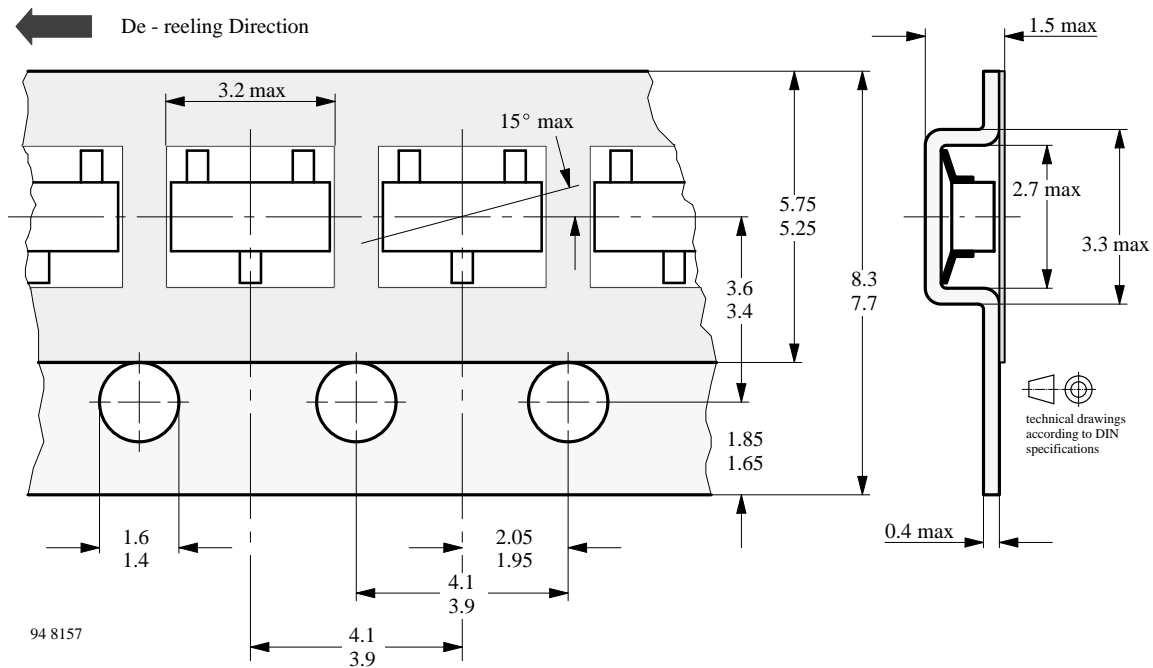


Figure 7.8 Tape dimensions in mm for SOT 23. The mounting side of the components is oriented to the bottom side in the tape.

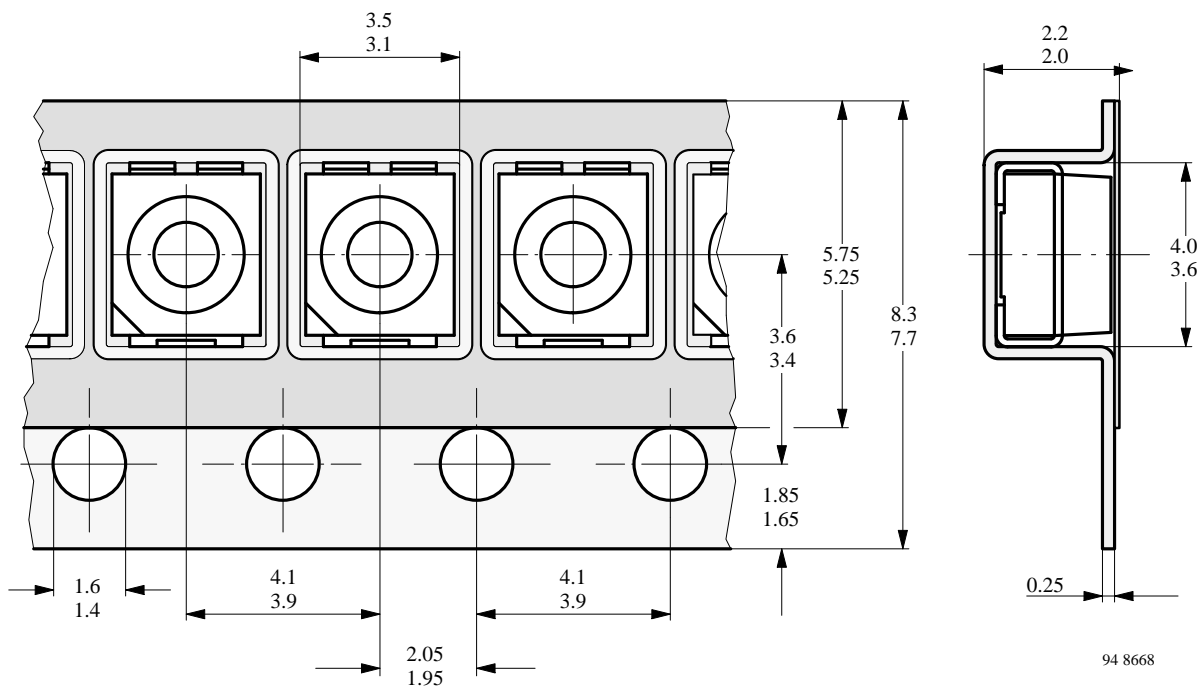


Figure 7.9 Tape dimensions in mm for PLCC2

### 7.3.1 Number of components

Quantity per reel in SOT 23 package: 3000 pcs

PLCC2 (Tantal B) package: 1500 pcs (minimum quantities for order)

## 7.3.2 Missing devices

Maximum of 0.5% of the total number of components per reel may be missing, exclusively missing

components at the beginning and at the end of the reel. Maximum of three consecutive components may be

missing, provided this gap is followed by six consecutive components.

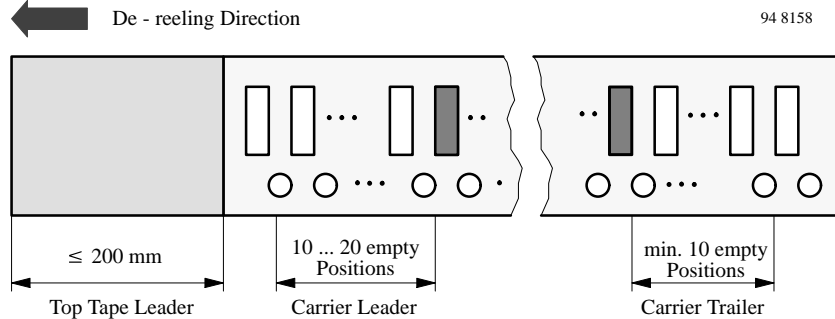


Figure 7.10 Beginning and end of reel

The top tape leader is at least 200 mm and is followed by a carrier tap leader with at least 10 and not more than 20 empty positions. The top tape leader

may include the carrier tape providing the two are not connected together.

carrier tape trailer with at least 10 empty positions, with the top tape attached to the carrier tape.

The last component is followed by a

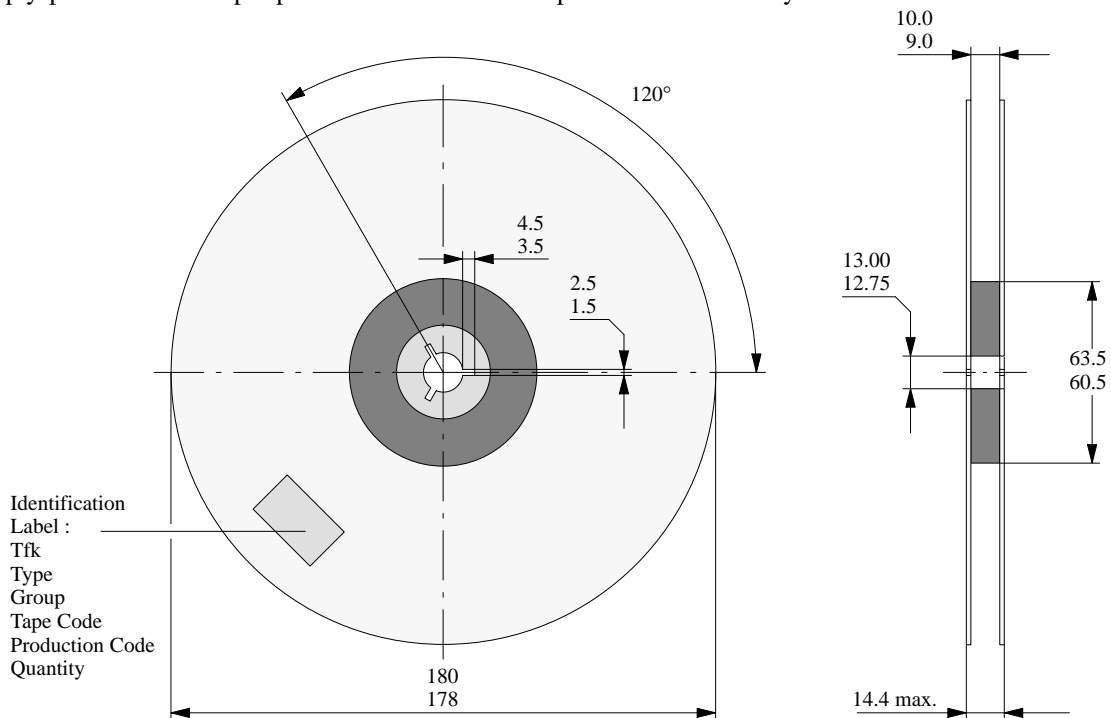


Figure 7.11 Dimensions of the reel

## 7.3.3 Top tape removal force

The removal force lies between 0.1 N and 1.0 N at a removal speed of 5 mm/s.

In order to prevent the components

from popping out of the blisters, the top tape must be pulled off at an angle of 180°C with respect to the feed direction.

The type designation of the device in SMT 23 package is extended by the code GS08.

**Example:** TEMD 2100 GS08

## 7.3.4 Ordering designation



## 8. Assembly instructions

### 8.1 General

Optoelectronic semiconductor devices can be mounted in any position. Connection wires may be bent provided the bend is not less than 1.5 mm from the bottom of the case. During bending, no forces must be transmitted from the pins to the case (e.g. by spreading the pins).

If the device is to be mounted near heat generating components, then consideration must be given to the resultant increase in ambient

temperature.

### 8.2 Soldering instructions

Protection against overheating is essential when a device is being soldered. It is recommended, therefore, that the connection wires are left as long as possible. The time during which the specified maximum permissible device junction temperature is exceeded at the soldering process should be as short as

possible (one minute maximum). In the case of plastic encapsulated devices, the maximum permissible soldering temperature is governed by the maximum permissible heat that may be applied to the encapsulant rather than by the maximum permissible junction temperature.

The maximum soldering iron (or solder bath) temperatures are given in Tab. 8.1. During soldering, no forces must be transmitted from the pins to the case (e.g. by spreading the pins).

Table 8.1 Maximum Soldering Temperatures

Iron soldering				Wave or reflow soldering		
	Iron temperature	Distance of the soldering position from the lower edge of the case	Maximum allowable soldering time	Soldering temperature <small>see temperature/time profiles</small>	Distance of the soldering position from the lower edge of the case	Maximum allowable soldering time
Devices in metal case	$\cong 245^{\circ}\text{C}$	$\cong 1.5\text{ mm}$	5 s	$245^{\circ}\text{C}$	$\cong 1.5\text{ mm}$	5 s
	$\cong 245^{\circ}\text{C}$	$\cong 5.0\text{ mm}$	10 s	$300^{\circ}\text{C}$	$\cong 5.0\text{ mm}$	3 s
	$\cong 350^{\circ}\text{C}$	$\cong 5.0\text{ mm}$	5 s			
Devices in plastic case $\geq 3\text{ mm}$	$\cong 260^{\circ}\text{C}$	$\cong 2.0\text{ mm}$	5 s	$235^{\circ}\text{C}$	$\cong 2.0\text{ mm}$	8 s
	$\cong 300^{\circ}\text{C}$	$\cong 5.0\text{ mm}$	3 s	$260^{\circ}\text{C}$	$\cong 2.0\text{ mm}$	5 s
Devices in plastic case $< 3\text{ mm}$	$\cong 300^{\circ}\text{C}$	$\cong 5.0\text{ mm}$	3 s	$260^{\circ}\text{C}$	$\cong 2.0\text{ mm}$	3 s

### Soldering Methods

There are several methods in use to solder devices on to the substrate. The following is not given as a complete list.

#### (a) Soldering in the vapor phase

Soldering in saturated vapor is also known as condensation soldering. This soldering process is in use as a batch system (dual vapor system) or as a continuous single vapor system. Both systems may also include a preheating of the assemblies to prevent high temperature shock and other undesired effects.

#### (b) Infrared soldering

With infrared (IR) reflow soldering the heating is contact-free and the energy for heating the assembly is derived from direct infrared radiation and from convection.

The heating rate in an IR furnace depends on the absorption coefficients of the material surfaces and on the ratio of component's mass to  $A_s$  irradiated surface.

The temperature of parts in an IR furnace, with a mixture of radiation and convection, cannot be determined in advance. Temperature measurement may be performed by

measuring the temperature of a certain component while it is transported through the furnace.

The temperatures of small components, soldered together with larger ones, may rise up to  $280^{\circ}\text{C}$ .

Influencing parameters on the internal temperature of the component are as follows:

- Time and power
- Mass of the component
- Size of the component
- Size of the printed circuit board
- Absorption coefficient of the surfaces
- Packing density
- Wavelength spectrum of the radiation source
- Ratio of radiated and convected energy

Temperature/time profiles of the entire process and the influencing

parameters are given in figure 8.1.

**(c) Wave soldering**

In wave soldering one or more continuously replenished waves of molten solder are generated, while the substrates to be soldered are moved in one direction across the crest of the wave.

Temperature/time profiles of the entire process are given in figure 8.2.

**(d) Iron soldering**

This process is essentially uncontrolled. It should not be considered for use in applications where reliability is important. There

is no SMD classification for this process.

**(e) Laser soldering**

This is an excess heating soldering method. The energy absorbed may heat the device to a much higher temperature than desired. There is no SMD classification for this process at the moment.

**(f) Resistance soldering**

This is a soldering method which uses temperature controlled tools (thermodes) for making solder joints. There is no SMD classification for this process at the moment.

## Temperature-Time-Profiles

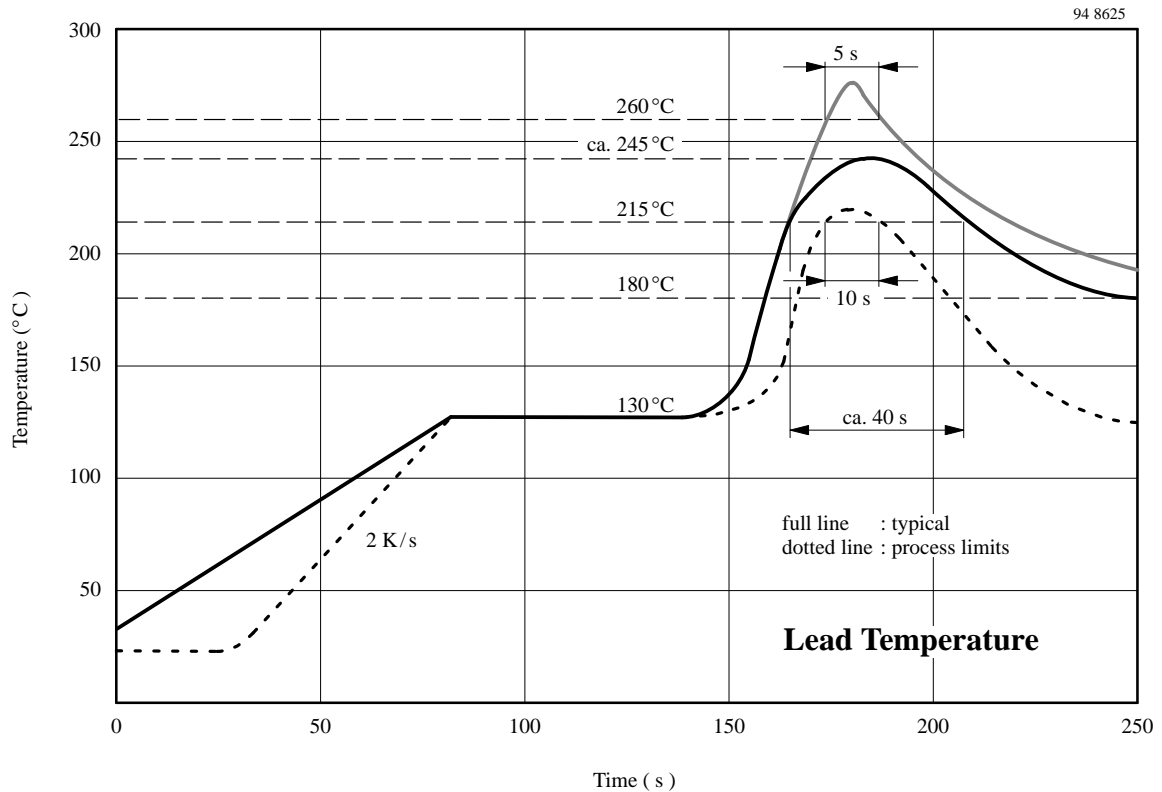


Figure 8.1 Infrared reflow soldering opto-devices (SMD package)

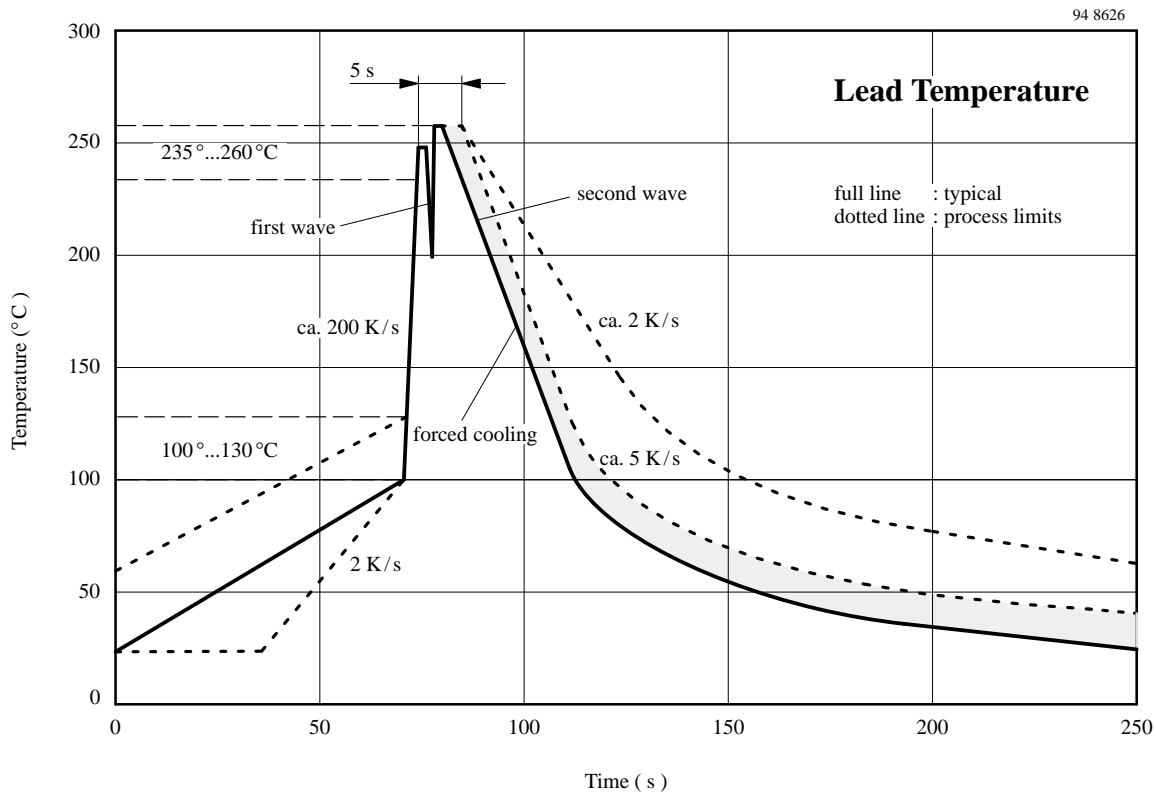


Figure 8.2 Wave soldering double wave opto-devices

### 8.3 Heat removal

To keep the thermal equilibrium, the heat generated in the semiconductor junction(s) must be removed and the junction returned to ambient temperature.

In the case of low power devices, the natural heat conductive path between the case and surrounding air is usually adequate for this purpose. The heat generated in the junction is conveyed

$$P_{\text{tot max}} = \frac{T_{\text{jmax}} - T_{\text{amb}}}{R_{\text{thJA}}} = \frac{T_{\text{jmax}} - T_{\text{amb}}}{R_{\text{thJC}} + R_{\text{thCA}}}$$

where:

$T_{\text{jmax}}$  the maximum allowable junction temperature

$T_{\text{amb}}$  the highest ambient temperature likely to be reached under the most unfavorable conditions

$R_{\text{thJC}}$  the thermal resistance, junction case

$R_{\text{thJA}}$  the thermal resistance,

to the case or header by conduction rather than convection. A measure of the effectiveness of heat conduction is the inner thermal resistance or thermal resistance junction case,  $R_{\text{thJC}}$ , the value of which is governed by the construction of the device.

Any heat transfer from the case to the surrounding air involves radiation convection and conduction, the effectiveness of transfer being

junction ambient, is specified for the components.

The following diagram shows how the different installation conditions effect the thermal resistance

$R_{\text{thCA}}$  the thermal resistance, case ambient.  $R_{\text{thCA}}$

depends on cooling conditions. If

expressed in terms of an  $R_{\text{thCA}}$  value, i.e., the external or case ambient thermal resistance. The total thermal resistance, junction ambient is consequently:

$$R_{\text{thJA}} = R_{\text{thJC}} + R_{\text{thCA}}$$

The total maximum power dissipation,  $P_{\text{tot max}}$  of a semiconductor device can be expressed as follows:

a heat dissipator or sink is used, then  $R_{\text{thCA}}$  depends on the thermal contact between case and heat sink, heat propagation conditions in the sink and the rate at which heat is transferred to the surrounding air.

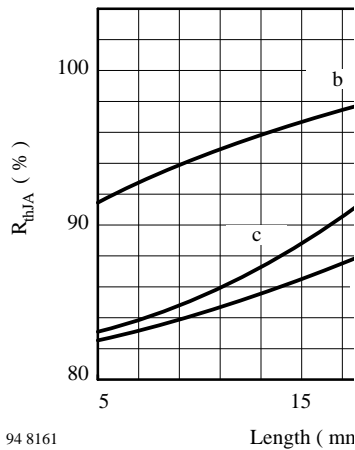
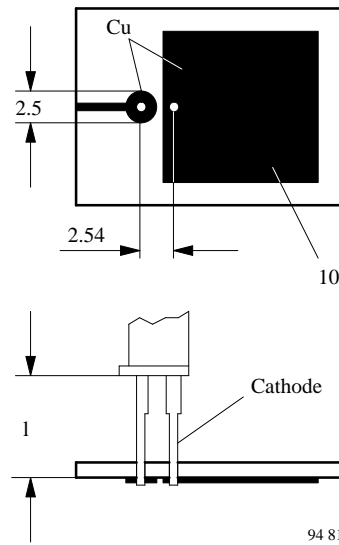


Figure 8.3 Thermal resistance junction/ambient vs. lead length



Commercially available grades (industrial use) shall be used.

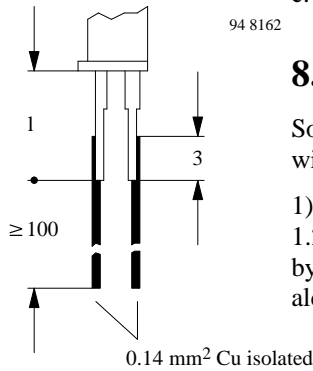
Warning: The component 1, 1,2-trichlorofluoroethane is hazardous to the environment. Therefore this solvent must not be used where the solvent specified in 2 or 3 is adequate.

2) 2-propanol (isopropyl alcohol). Commercially available grades (industrial use) should be used.

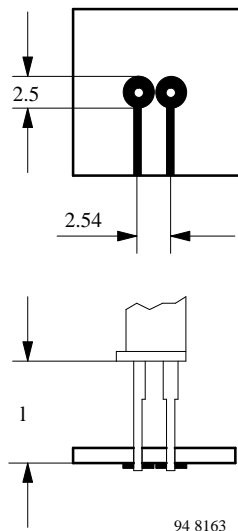
3) Demineralized or distilled water having a resistivity of not less than 300 mΩ corresponding to a conductivity of 2 mS/m.

**Caution:** The use of tetrachlor, acetone, trichloroethylene or similar is **NOT ALLOWED!**

c. with PC board with heatsink



a. with wires



b. with PC board without heatsink

## 8.4 Cleaning

Soldered assemblies are washable with the following solvents:

- 1) A mixture of 1, 1,2-trichlorotrifluoroethane, 70 ± 5% by weight and 2-propanol (isopropyl alcohol), 30 ± 5% by weight.

## 8.5 Warning

Exceeding any one of the ratings (soldering, cleaning or short time exceeding the railings) could result in irreversible changes in the ratings.